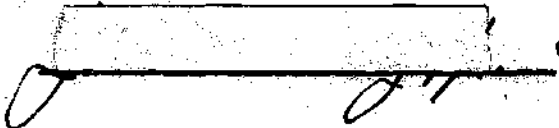


"In presenting the dissertation as a partial fulfillment of the requirements for an advanced degree from the Georgia Institute of Technology, I agree that the Library of the Institution shall make it available for inspection and circulation in accordance with its regulations governing materials of this type. I agree that permission to copy from, or to publish from, this dissertation may be granted by the professor under whose direction it was written, or, in his absence, by the dean of the Graduate Division when such copying or publication is solely for scholarly purposes and does not involve potential financial gain. It is understood that any copying from, or publication of, this dissertation which involves potential financial gain will not be allowed without written permission.



INVESTIGATION OF CERTAIN ASPECTS OF
METEOR-BURST PROPAGATION

A THESIS

Presented to
the Faculty of the Graduate Division

by

John Broadus Berry, Jr.

In Partial Fulfillment
of the Requirements for the Degree
Master of Science in Electrical Engineering


Georgia Institute of Technology

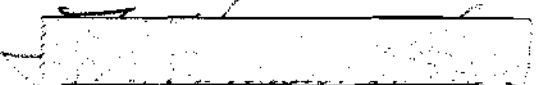
December, 1959

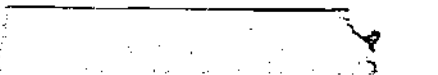
58
12R

INVESTIGATION OF CERTAIN ASPECTS OF
METEOR-BURST PROPAGATION

Approved:


W. B. Jones, Jr


F. Kenneth Hurd


E. W. McDaniel

Date Approved by Chairman: Dec. 11, 1959

ACKNOWLEDGEMENTS

The work reported here was supported principally by the Air Force Cambridge Research Center under Contract No. AF 19(604)-5187. The experimental data were obtained under Contract No. AF 19(604)-1593. The contributions to the work by members of the staff of the Engineering Experiment Station of the Georgia Institute of Technology are gratefully acknowledged. In particular, the author acknowledges the assistance and patience of my thesis advisor, Dr. W. B. Jones, Jr. and the inspiration and guidance of Dr. M. L. Meeks, who is now on the staff of Harvard College Observatory. A special note of appreciation is due Miss Alma Joyce Rice and Mr. A. P. Jensen for their contributions in data processing and computer programming, respectively.

TABLE OF CONTENTS

	Page
ACKNOWLEDGEMENTS	ii
LIST OF TABLES	iv
LIST OF ILLUSTRATIONS	v
SUMMARY	vii
Chapter	
I. INTRODUCTION	1
II. THEORY	6
Exponent k	6
Decay Time Constant (τ)	13
III. INSTRUMENTATION AND DATA PROCESSING	17
IV. DISCUSSION OF RESULTS	25
Duty Cycle Versus Decision Levels	25
Distribution of Decay Constants	42
V. CONCLUSIONS	49
VI. RECOMMENDATIONS	53
APPENDIX I. CALCULATION OF SYSTEM RESPONSE	55
APPENDIX II. SAMPLE CALCULATION BASED ON FITTING OBSERVED DATA TO A TRUE EXPONENTIAL	59
BIBLIOGRAPHY	63

LIST OF TABLES

Table	Page
1. Characteristics of Two Meteor Scatter Paths	17
2. Characteristic Meteor Echo Signal Shapes	21

LIST OF ILLUSTRATIONS

Figure	Page
1. Block Diagram of a Typical Meteor-Burst Communication System	3
2. Theoretical Meteor Echo From an Underdense Trail	15
3. Measured Overall System Transient Response, Congaree, March 22, 1958	19
4. System Transient Response Replotted on Rectilinear Coordinates Showing Equivalent Time Constants	19
5. Examples of Three Types of Meteor Echoes: (A) Specular Underdense, (B) Specular Overdense, (C) Non-Specular Overdense	22
6. Duty Cycle as a Function of Receiver Decision Level as Scaled from Edin Data	26
7. Duty Cycle as a Function of Receiver Decision Level as Scaled from Edin Data	27
8. Duty Cycle as a Function of Receiver Decision Level as Scaled from Edin Data	28
9. Duty Cycle as a Function of Receiver Decision Level as Scaled from Edin Data	29
10. Duty Cycle as a Function of Receiver Decision Level as Scaled from Edin Data	30
11. Duty Cycle as a Function of Receiver Decision Level as Scaled from Edin Data	31
12. Duty Cycle as a Function of Receiver Decision Level as Scaled from Edin Data	32
13. Duty Cycle as a Function of Receiver Decision Level as Scaled from Edin Data	33
14. Comparison of Duration and Numerical Data	34
15. Comparison of Duration and Numerical Data	35

LIST OF ILLUSTRATIONS (Continued)

Figure	Page
16. Duty Cycle as a Function of Receiver Decision Level as Measured by the UF/MSA-1 Meteoric Signal Analyzer	36
17. Distribution of Meteor Echo Decay Time Constants. 49 mc Morning (0400 - 0900 EST), 317 Cases	43
18. Distribution of Meteor Echo Decay Time Constants. 74 mc Morning (0400 - 0900 EST), 524 Cases	44
19. Distribution of Meteor Echo Decay Time Constants. 49 mc Evening (1700 - 2000 EST), 86 Cases	45
20. Distribution of Meteor Echo Decay Time Constants. 74 mc Evening (1700 - 2000 EST), 133 Cases	46
21. Bandwidth-Frequency Considerations on a Typical Meteor-Burst Radio Link	51
22. Theoretical Effect of Finite System Response Time on an Exponential Decay Signal	56

SUMMARY

The purpose of this research was to measure two functions of importance to meteor-burst communications which have not previously been clearly defined: (1) the dependence of integrated signal durations on receiver decision level and (2) the distributions of and diurnal variations in meteor echo decay time constants. These investigations were based on data obtained during eleven months of operation of two typical meteor-burst radio links.

If only the echoes from specular underdense meteor trails are considered, the relationship between relative signal time D_0 and the receiver threshold amplitude A_0 is of the form

$$D_0 = \frac{\text{Constant}}{A_0^k} .$$

The exponent k was found to have a value of approximately unity. This value agrees with theory and the observed meteoritic mass distribution. Measurements based on contributions of other types of echoes also showed exponential characteristics but with exponents greater than unity. Apparently, previously reported measurements of this exponent included contributions by all types of echoes and signals. This could account for the wide range of values encountered.

It has been shown theoretically that the information rate, I , which can be transmitted over a meteor-burst communication link is related to the bandwidth B by

$$I = \text{Constant} \times B^{\frac{2-k}{2}}$$

If the exponent k is less than 2, then maximum I can be achieved with maximum bandwidth. The values of k measured in this study are shown in the following summary:

<u>type of signals</u>	<u>values of k measured</u>
specular underdense only	1.06 ± 0.24
all specular echoes	1.37 ± 0.34
all signals	1.15 to 1.84

Since all values measured were less than the critical value of 2.0 it was concluded that the average information rate on a meteor-burst communications system of this type may be optimized by using as large a bandwidth as feasible.

The measurements upon which these conclusions are based were made over two similar experimental radio links and two operating frequencies of 49 and 74 megacycles per second. The integrated signal durations are presented in terms of duty cycle (which is the term commonly used in discussions of practicable systems). These results may be extrapolated over a reasonable range of frequencies and signal levels but extension beyond about 300 megacycles is not advised. Additional measurements over other transmission paths and frequencies are recommended to confirm these results and extend the results to other conditions.

The distribution of meteor echo decay time constants was measured on both frequencies and at two critical times of day. The observed decay shapes were fitted to a true exponential by the method of least squares as programmed on a digital computer. The computed time constants were

carefully screened for poor exponential fits and other distortions such as might be caused by multipath fading.

The results show that rather wide variations in the values of τ are to be expected. The median values seem to indicate that the majority of meteor echoes of this type occur at altitudes slightly higher than was expected. The evening median was greater than the early morning value by a factor of about 1.55. This effect was predicted by consideration of the effect of the earth's heliocentric velocity. Measurements of the effect of wavelength on decay time constants were inconclusive.

The values obtained in measurements of the decay time constants are valid only over the paths and frequencies used. Additional measurements are recommended to determine the median values to be expected on other frequencies and with variations in the other parameters.

CHAPTER I

INTRODUCTION

In meteor-burst communication systems the maximum information rate depends upon the relationship between relative signal duration (or "duty cycle") and receiver decision level. The distribution of meteor echo decay time constants and diurnal fluctuations in the distribution also affect the information rate and system design parameters. These aspects of meteor-burst propagation are studied in detail here using data from two typical meteor-burst radio links described in Chapter III.

A meteor-burst communication system uses ionized trails caused by meteors as passive reflectors to extend the useful range of VHF* radio beyond the horizon. An ionized trail is caused as a particle of solar system dust enters the earth's atmosphere at speeds up to 72 kilometers per second at a height of about 100 kilometers above the earth's surface. The long thin column of ionization called a meteor "trail" diffuses rapidly at this height and a typical trail supports reflection for only a fraction of a second. The number of such meteor trails is very large, in the order of billions per day, and this rate of trail formation compensates to a large extent the short life of a typical trail. To be useful as a reflector, the trail must contain enough ionization to support

*Very High Frequency is defined as that part of the radio spectrum from 30 to 300 megacycles per second.

at least partial reflection and it must be properly oriented geometrically to reflect a signal from the transmitter to the receiver. Trails with initial electron line densities sufficient to support only partial reflection are called "underdense" trails. The radio signal reflected by such a trail is referred to as an underdense signal or echo. Trails which will support complete reflection are referred to as "overdense" and radio signals thus reflected are called overdense signals or echoes. A typical 5 kilowatt, 1200 kilometer radio link will detect about five trails per minute.

Figure 1 shows a block diagram of a typical meteor-burst communication system. Both transmitters operate continuously with information modulation only when a closed two-way path exists. The appearance of a suitably oriented meteor trail causes a burst of signal at both receivers. Gating signals are generated which cause each transmitter to transmit station identification. This is received and acted upon at the distant stations as indication of a closed loop. Information flow begins in both directions at a high speed consistent with bandwidth and signal-to-noise ratio. Stopping the information flow without error is a major problem. Most commonly a minimum signal-to-noise criteria at each receiver is used to start a "stop" pattern. When this minimum decision level is reached by either receiver information flow in one direction ceases and a "stop sending" code is transmitted. At the distant station the reception of a stop sending code gates the transmitter to standby removing information modulation and information flow is thus concluded in both directions. Detailed system arrangements are described in the literature.^{1,2,3}

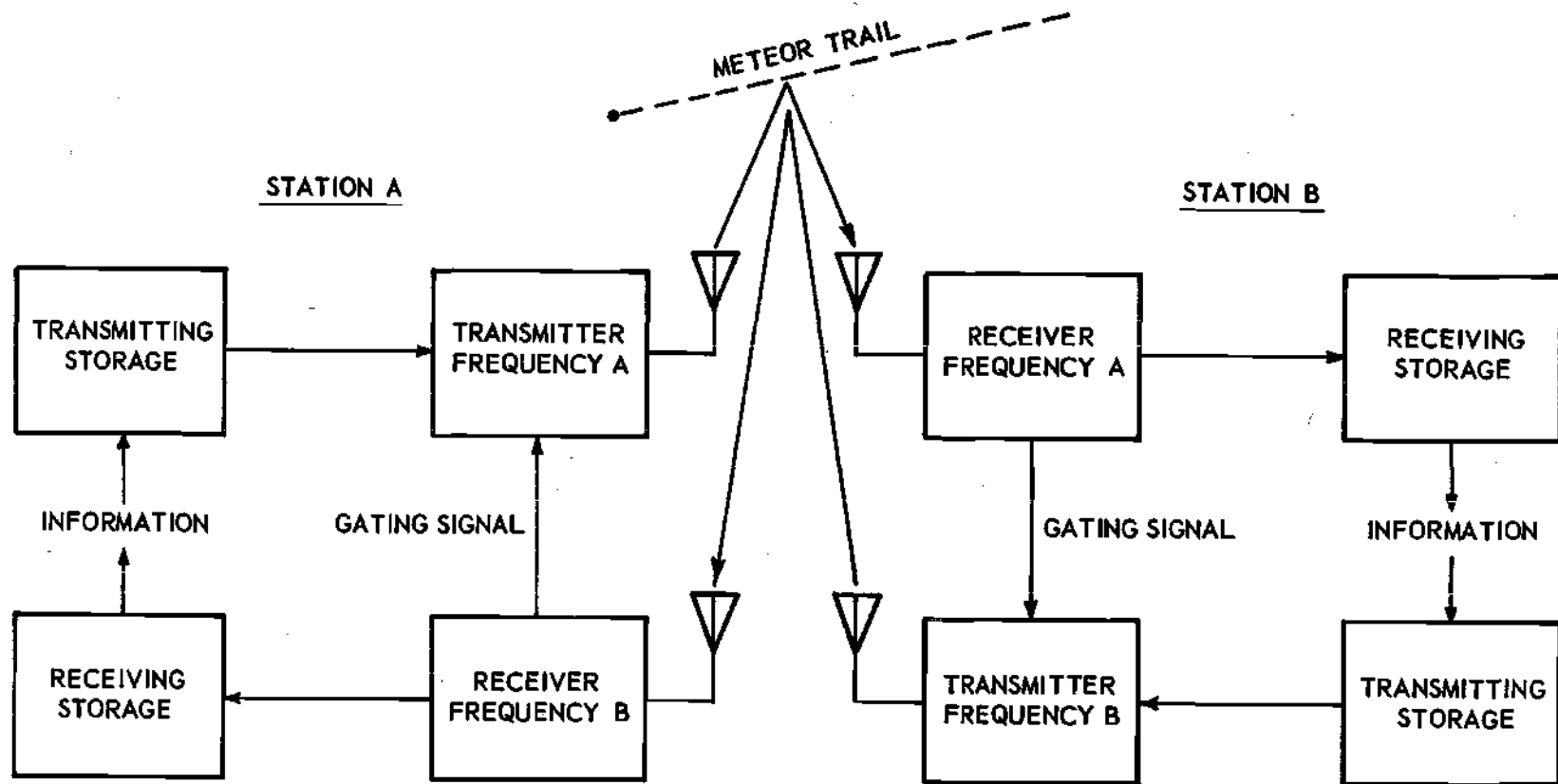


Figure 1. Block Diagram of a Typical Meteor-Burst Communication System.

In Chapter II it is shown that the average information rate for underdense signals has the form

$$I = C_4 B^{\frac{2-k}{2}} \quad S/N = \text{Constant} \quad (19)$$

where

I is the average information rate,

C_4 is a constant lumping a number of terms,

B is the system bandwidth,

k is an exponent in the duty-cycle versus receiver decision level relationship, and

S/N is the signal-to-noise ratio at threshold A_0 .

From (19) it is apparent that the maximum of the average information rate occurs at maximum bandwidth if k is less than 2. Previous measurements by others have obtained values of k ranging from 1.3 to 2.7.⁴ The theory discussed in Chapter II shows that for the more numerous specular underdense signals a value of $k = 1$ should be obtained. The value of this exponent k as a function of the various types of signals encountered is an important consideration in the design of the meteor-burst communication system.

The importance of further measurement of the exponent k was discussed by Vincent *et al.*⁴ It appears that previous measurements of k did not take into account the effect of each of the three types of signals. In the investigation reported herein and discussed in Chapter IV a value of k is obtained consistent with theory when the nonspecular and overdense signals are excluded.

The possibility of longer enduring signals during the early evening hours is predicted on the basis of the slower velocities encountered on the antapex side of the earth. Forsyth et al., mention this effect and propose that it might help to compensate, to some extent, for the lower meteor rate at this time of day.¹ The distribution of meteor echo decay time constants measured at approximately 0600* and 1800 hours local time are reported herein to confirm and evaluate this effect.

There is very little literature available on the distribution of meteor echo decay time constants on a typical forward scatter meteor system. Wirth reports a distribution which has the same overall shape as was obtained here with a median close to the value expected at 43.5 megacycles.⁵ However, a "best-fit" method for determining τ was not used and a single measurement at $1/e A_p$ is of questionable value due to trail distortion. The author questions his own results and suggests further measurements. The diurnal variation in the shape of this distribution probably contributes to the inaccuracy of his result.

* All times are expressed in the 24 hour notation beginning at 0000 (midnight) local time.

CHAPTER II

THEORY

Exponent k.—The number and mass distribution of sporadic meteors over a wide range of masses has been observed to be of the form

$$dN = \frac{dM}{M^p} \quad (1)$$

where N is the number of meteors, M is the meteoroid mass before ablation and p is an exponent with a value of approximately 2, obtained from many measurements.^{6,7} The generation of free electrons in the trail is given by

$$q_{\max} = \frac{4}{9} \gamma (\mu H)^{-1} M \cos z \quad (2)$$

where q_{\max} is the maximum electron line density along the trail, γ is the probability that an evaporated meteor atom will produce an ion pair, μ is the mean mass of an evaporated atom, H is the scale height, M is the meteoroid mass, and z is the zenith angle of the trail axis.^{8,9}

For a communication system utilizing meteor trail reflection the relationship between received power P_R and the ionization density q of a long thin meteor trail is expressed by Eshleman's equation for the forward scatter case as

$$P_R = \frac{P_T}{16\pi^4} \left(\frac{\mu_o q_e^2}{4m_e} \right)^2 \frac{\lambda^3}{R_1 R_2 (R_1 + R_2)} \frac{G_R G_T q^2 s^2}{1 - \cos^2 \beta \sin^2 \phi} \exp\left(\frac{32\pi^2 D t}{\lambda^2 \sec^2 \phi} \right) \quad (3)$$

where

P_R and P_T are the received and transmitted powers,

μ_0 is the permeability of free space,

q_e and m_e are the charge and mass of an electron,

λ is the radio wavelength,

R_1 and R_2 are distances from the center of the trail's first Fresnel zone to the transmitter and receiver,

G_T and G_R are antenna gains in the direction of the trail,

ϕ is $1/2$ the enclosed angle between R_1 and R_2 ,

S is a polarization factor,

β is the angle between the axis of the meteor trail and the transmitter-receiver-meteor plane,

D is the ambipolar diffusion coefficient,

t is the time elapsed since the formation of the trail,

and

q is the line charge density. (all in MKS units)

This equation holds only so long as the trail ionization density q is below a critical value q_0 of approximately 10^{14} electrons per meter of line charge above which the trail acts as a metallic cylinder and supports complete reflection.¹⁰ As q exceeds q_0 the peak reflected power increases only very slowly but the time duration of the echo increases.

The majority of the meteor echoes observed by radio techniques are from trails of q less than q_0 which are called "underdense" trails. The case of q greater than q_0 leads to what is called an "overdense" trail. The derivations that follow apply only to echoes caused by underdense trails.

From (3) it follows that

$$P_R = f(q^2) \text{ or}$$

$$A = f(q)$$

where A is the amplitude of the received meteor echo. Then

$$A_p = f(q_{\max}) \quad (4)$$

where A_p is the peak echo amplitude. From (2) it is seen that q_{\max} is a function of the original meteoroid mass M ; therefore the received peak amplitude A_p can be expressed as a function of the meteoroid mass M for any properly formed trail

$$A_p = f(M) \quad (5)$$

If a typical forward scatter meteor-burst system is operated for a sufficient length of time to receive echoes from a wide variety of meteors, geometrical and probability quantities such as γ , H , z , R_1 , R_2 , S , β , and ϕ would be expected to average out or become constants when integrated over time. After such an averaging process (5) can be substituted in (1)

$$dN = C \frac{dA_p}{A_p}$$

To find the total number of maximum amplitudes above any threshold amplitude A_0 an integration over all amplitudes greater than A_0 is performed,

$$N_o = C \int_{A_o}^{\infty} \frac{dA}{A^p}$$

$$N_o = \frac{C}{(p-1)(A_o^{p-1})}, \quad p > 1. \quad (6)$$

For an observed value of $p = 2$, (6) simplifies to the form in which it is most often seen

$$N_o = \frac{C}{A_o}, \quad p = 2 \quad (7)$$

(an inverse law relationship) where

N_o is the number of underdense echoes of maximum amplitude greater than A_o , and

C is a constant of proportionality.

Because of the importance of the exponent of A_o in predicting system performance (7) is frequently written in the form

$$N_o = \frac{C}{A_o^k} \quad (8)$$

where $k = p-1$.

The total signal duration D_o of underdense meteor echoes at any receiver decision threshold level A_o is

$$D_o = \int_{A_o}^{\infty} N(A) T(A) dA \quad (9)$$

where $N(A)$ is the number of maximum amplitudes A in the interval $A, A + dA$ and $T(A)$ is the duration of an echo of maximum amplitude A at

the threshold A_0 . The integration is to be performed over amplitudes and not time, therefore the notation A infers peak echo amplitude. If the signals are underdense and have a mean decay time constant of τ the exponential

$$A = A_p e^{-\frac{t}{\tau}}, \quad t \geq 0 \quad (10)$$

can be used to describe the average echo shape.*

In (9) $T(A)$ has been defined as the duration at A_0 so (10) may be written in the form

$$A_0 = A e^{\frac{T(A)}{\tau}}, \quad T(A) \geq 0. \quad (11)$$

Solving for $T(A)$

$$T(A) = \tau \ln \frac{A}{A_0}. \quad (12)$$

$N(A)$ is the first derivative of N_0 in (8) with respect to an incremental range of amplitude dA

$$N(A) = \frac{dN_0}{dA} = C \frac{dA^{-k}}{dA}$$

$$N(A) = CkA^{-(k+1)}. \quad (13)$$

Substituting (12) and (13) in (9) and performing the integration

* See Equation (21) in this same chapter.

$$\begin{aligned}
D_o &= \int_{A_o}^{\infty} CkA^{-(k+1)} \tau \ln \frac{A}{A_o} dA \\
&= k\tau C \int_{A_o}^{\infty} A^{-(k+1)} [\ln A - \ln A_o] dA \\
D_o &= k\tau C \left[\int_{A_o}^{\infty} A^{-(k+1)} \ln A dA - \int_{A_o}^{\infty} A^{-(k+1)} \ln A_o dA \right] \\
&= k\tau C \left[A^{-k} \left(\frac{\ln A}{-k} - \frac{1}{k^2} \right) \right]_{A_o}^{\infty} - k\tau \ln A_o \left[\frac{A^{-k}}{-k} \right]_{A_o}^{\infty} \\
&= k\tau C \left[A_o^{-k} \frac{\ln A_o}{k} + \frac{A_o^{-k}}{k^2} - A_o^{-k} \frac{\ln A_o}{k} \right].
\end{aligned}$$

The first and last terms cancel, yielding

$$D_o = \frac{C\tau}{kA_o^k} \quad (14)$$

which is the functional dependence of the relative total signal duration or "duty cycle" on receiver decision level for underdense echoes.

The result expressed in (14) can be utilized to derive the system information rate. The average information rate I of a meteor burst system is given by¹

$$I = (\text{instantaneous rate}) \times (\text{duty cycle}).$$

If the instantaneous rate is assumed to be proportional to bandwidth this may be written

$$I = C_1 B D_o \quad (15)$$

where I is the mean information rate corresponding to receiver decision level A_0 , C_1 is a constant of proportionality relating instantaneous information rate and bandwidth B , and D_0 is given by (14) for underdense echoes.¹¹ Substituting (14) in (15) gives

$$I = C_1 B \frac{C_T}{k A_0^k} \quad (16)$$

The bandwidth factor B is dependent on receiver decision level A_0 for any constant signal-to-noise ratio S/N at this threshold. For a constant signal-to-noise ratio at threshold A_0 , B may be written

$$B = C_2 A_0^2, \quad S/N = \text{constant} \quad (17)$$

where C_2 is a constant of proportionality. Combining (16) and (17)

$$I = C C_1 C_2 \left(\frac{I}{k}\right) \frac{A_0^2}{A_0^k}, \quad S/N = \text{constant}$$

$$I = C_3 A_0^{2-k}, \quad S/N = \text{constant} \quad (18)$$

where

$$C_3 = C C_1 C_2 \frac{I}{k}$$

Referring back to (17) the bandwidth factor may be reinserted in (18) to yield the final result

$$I = C_4 B^{\frac{2-k}{2}}, \quad S/N = \text{constant} \quad (19)$$

where C_4 is a constant lumping a number of terms. The importance of the numerical value of exponent k is emphasized by noting that when it is less than 2.0 maximum information rate occurs at maximum bandwidth B . The information rate is independent of bandwidth for a value of exactly 2.0 and minimum bandwidth gives optimum results if k is greater than 2.0. The numerical value may be measured experimentally from duration data that agree with the exponential form expressed by equation (14). It should be emphasized that (19) includes several assumptions and is valid only for underdense signals.

Decay time constant τ .—As a meteoroid enters the earth's atmosphere at speeds up to 72 kilometers per second, an ionized trail is formed by successive collisions with air molecules. The kinetic energy of each collision is sufficient to ablate material from the surface of the meteoroid. Each meteor atom thus released with a kinetic energy in the range of 100 to 1000 electron volts can ionize and excite nearby air particles.⁸ Experimental evidence indicates that the energy consumed in the meteoroid's deceleration is very small compared with the energy of ablation. It is therefore convenient to assume a constant velocity during the trail formation. It has also been found that the assumption of a long thin cylinder of ionization is valid for most meteor trails used in VHF forward scatter systems.

The trail must satisfy a certain geometrical condition to be useful as a reflector for a forward-scatter radio system.¹ The trail must be tangent to one of a family of prolate spheroids having the transmitter and receiver as common foci. This point of tangency must, of course, lie in the so-called meteor trail zone — approximately 100 kilometers above

the earth's surface. The tangent point also forms the center of the first Fresnel zone in the diffraction pattern which results as the meteor trail forms. If a trail is properly oriented when formed the resulting echo is "specular." Frequently a long-enduring trail which formed with an electron line density of greater than 10^{14} electrons per meter (overdense) will be twisted by upper-atmosphere winds to produce one or more points of reflection or "glints." The resulting echo is called "non-specular." Non-specular echoes are almost always caused by overdense trails since most underdense trails decay too rapidly to be disturbed appreciably by large scale turbulence.

Loewenthal has calculated the theoretical meteor echo shape using Fresnel integrals.¹² Figure 2 shows the shape to be expected for a meteor with a velocity of 70 kilometers per second traveling at right angles to the transmission path. A wavelength of 4 meters and a range of 600 kilometers correspond to an echo from an underdense trail formed at the midpoint of the Walpole-Congaree experimental radio link. Figure 2 was scaled from the results which Loewenthal plotted on normalized coordinates. The velocity and angle β were chosen to give the most rapid rise time and the highest Fresnel ripple frequency to be expected during the experiment.

Ignoring the Fresnel ripples the signal amplitude will decay in accordance with the exponential term in Eshleman's equation (3)

$$P_R(t) = P_R(\max) \exp\left(\frac{-32\pi^2 D t}{\lambda^2 \sec^2 \varphi}\right) \quad (20)$$

The amplitude of the signal as a function of time can be written

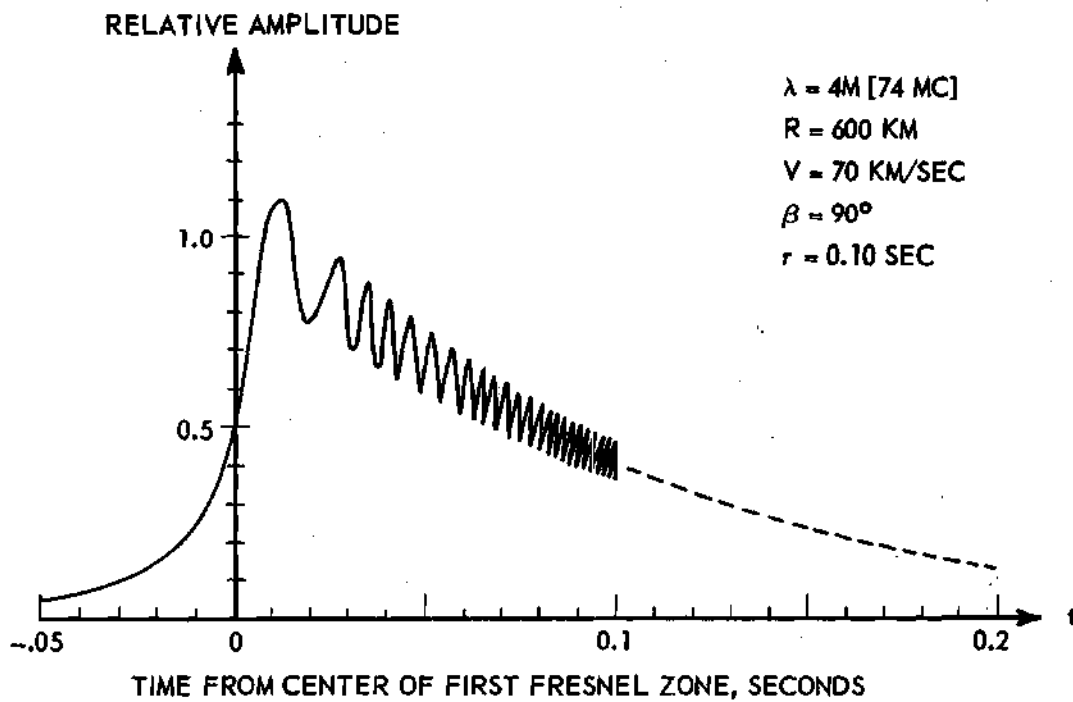


Figure 2. Theoretical Meteor Echo From an Underdense Trail.

$$A(t) = A_{\max} \varepsilon^{-\frac{t}{\tau}}, \quad t > 0 \quad (21)$$

where the decay time constant τ is given by

$$\tau = \frac{\lambda^2 \sec^2 \phi}{16 \pi^2 D} \quad (22)$$

In MKS units τ is the time in seconds until the meteor echo amplitude decays to $1/e$ of its maximum value.

A meteor burst communication system's antenna will normally illuminate a large area in the meteor trail zone and thus the distribution of decay time constants observed will depend upon the distribution of enclosed half-angles ϕ and also upon the diffusion coefficient D encountered by the ionized trails. If a given system is operated for a reasonable length of time it is possible to average out variations in the angle ϕ . The diffusion coefficient D encountered by the trail depends on the height above the earth's surface where the trail is formed. This in turn is a function of the energy of ablation of the meteoroid. Meteoroids of high velocity burn out at high altitudes where D is relatively large. The distribution of decay time constants τ will be strongly dependent on the distribution of meteor velocities for a given meteor-burst radio link.

CHAPTER III

INSTRUMENTATION AND DATA PROCESSING

The experimental data used in these studies were obtained over two transmission paths. The paths had a common origin at Walpole, Massachusetts with receiving and recording terminals located at Smyrna, Georgia and Congaree, South Carolina. The characteristics are shown in Table 1.

Table 1. Characteristics of Two Meteor Scatter Paths

	<u>Walpole - Smyrna</u>	<u>Walpole - Congaree</u>
Path Length	1480 KM	1250 KM
Frequencies Used	49.44 mc & 73.82 mc	49.44 mc & 73.82 mc
Transmitted Power		
49.44 mc	5 kw	5 kw
73.82 mc	3 kw	3 kw
Antennas		
Type	5 el Yagi	5 el Yagi
Gain Over Isotropic	11 db	11 db
Receiving System		
VHF Converter	N.B.S. Design	N.B.S. Design
5 mc Receiver	BC 779	SP 600 JX
Recorder	Edin, UF/MSA-1	Edin

A complete discussion of these radio links and related details is contained in the Final Report on Project A-263.¹³

The recorder used in the test was an Edin 6 channel direct writing instrument. The recorder frequency response was from zero to

approximately 30 cycles per second. The chart speed on this particular unit was accurate to better than one part in 360. The UF/MSA-1 electronic duty-cycle recorder is described in detail elsewhere.¹³ This is a threshold operated device in which the duty cycle measurement contains all types of signals. It was used only at the Smyrna site.

The effect of overall system response on the meteor echo shape is an important consideration in evaluating the recordings. The results of overall system tests are shown in Figures 3 and 4. Figure 3 shows the measured overall system transient response. A replot on rectilinear coordinates is shown in Figure 4. Since the receiver AVC voltage is approximately proportional to the logarithm of the input voltage over a large range a straight line is fitted to the response to emphasize the good fit to a logarithmic decay and rise. The equivalent decay time constant of the overall system used at Congaree was 0.008 seconds. The response of the Smyrna system was not measured but was similar in all respects to the Congaree system and was estimated to be approximately 0.01 seconds or better.

The calculations and graphs in Appendix I indicate that no measurable degradation of the meteor echo shape occurs for decay time constants τ of the order of about 0.04 seconds or greater due to measurement errors from other sources. For meteor decay time constants of the order of about 0.08 seconds or greater the finite system response is negligible in the presence of other trail distortions in determining the equivalent meteor decay time constant τ by the method of least squares.

The experimental radio links were operated for from 24 to 48 hours each week during the period August, 1957 to June, 1958. During most of

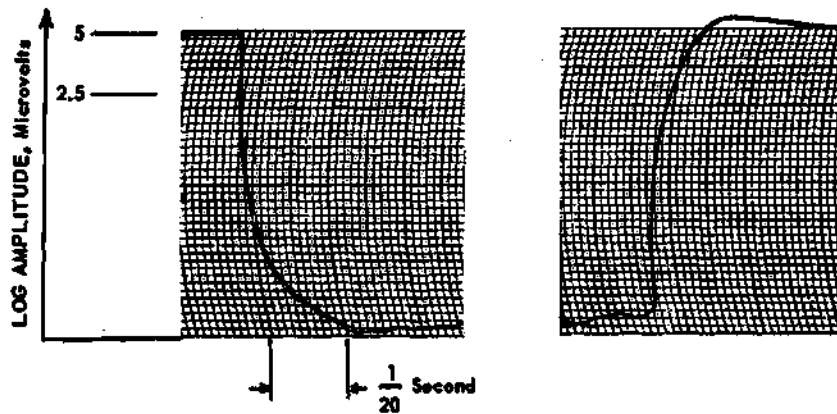


Figure 3. Measured Overall System Transient Response, Congaree March 22, 1958.

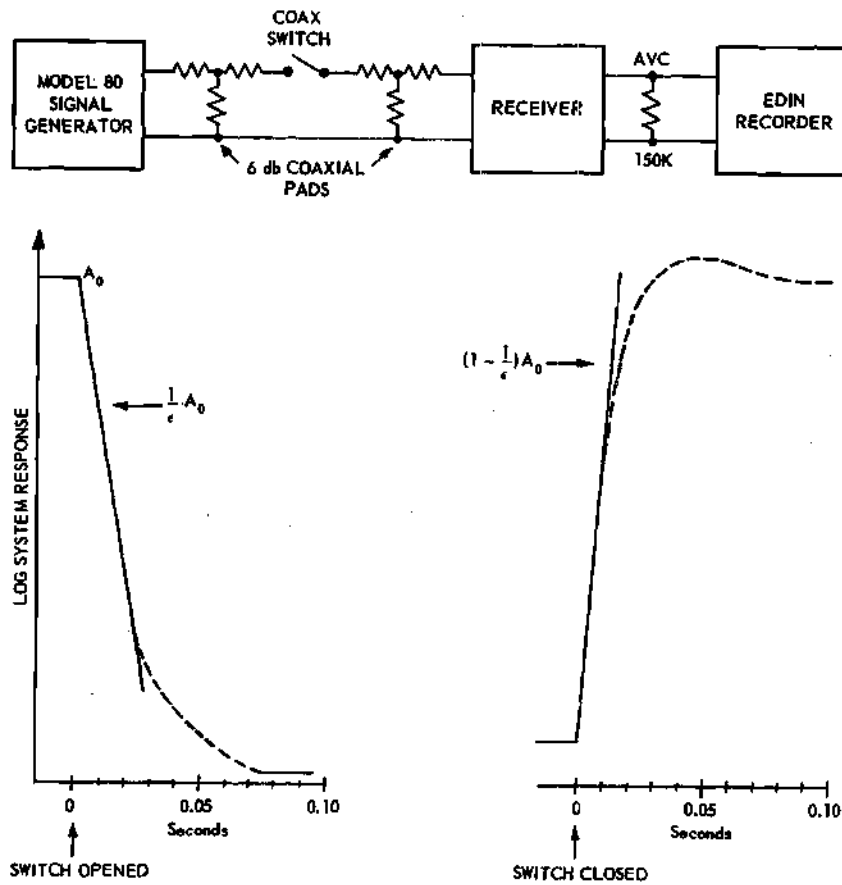


Figure 4. System Transient Response Replotted on Rectilinear Coordinates Showing Equivalent Time Constants.

each operation the Edin recorder was operated at 1 millimeter per second chart speed to observe meteor echo rates. However, for signal shape analysis, the chart speed was increased to 10 millimeters per second for 20 minutes at about 0600 and 30 minutes at about 1800 local time. In addition, high speed recordings were obtained at Congaree during the antenna spacing tests in May, 1958. At Smyrna, some miscellaneous high speed recordings were obtained in connection with monitoring of Sputnik I in October, 1957. Altogether, Project A-263 produced 1093 minutes of useable 10 millimeter per second Edin records. The majority of the charts contain two channels on each frequency.

The experiments described above were performed primarily for antenna siting studies. As a consequence the high-speed data were taken under varying antenna conditions. During any one high-speed run the antennas were fixed and the meteor echoes were recorded simultaneously on both frequencies and, in the case of Congaree, for both antenna arrangements. It is felt that the records represent a good cross-section of varying antenna and terrain conditions for a typical meteor scatter path.

All of the available Edin chart recordings were catalogued, indexed, and graded. The better sections of data were selected for further study. Poor or improper calibration, equipment failures, pen and inking troubles, thunderstorms, off-frequency operation, and similarly disturbed data were rejected.

Meteor propagated signals are generally classified by shape into three categories — specular underdense, specular overdense, and non-specular overdense. These terms agree with the theory discussed in Chapter II. The characteristics of each are given in Table 2.

Table 2. Characteristic Meteor Echo Signal Shapes

<u>Classification</u>	<u>Characteristic Shape</u>
Specular Underdense	Fast rise to a sharp peak followed by an immediate exponential decay.
Specular Overdense	Fast rise to a broad peak and an exponential decay sometimes distorted by fading.
Non-Specular Overdense	Slow rise to a broad peak and slow decay usually highly distorted by fading.

Examples of each type of signal are shown in Figure 5. A great many signals at first glance do not seem to clearly fit in any single category. For the most part they can be accurately classified if the disturbing factors such as fading and simultaneous signals are ignored.

During the transmission tests each channel was calibrated every 4 hours. In addition, the receiving converter input was terminated in a 50 ohm resistive load once each hour. Calibration strips consisting of a paper strip with threshold marks were made up for each high speed run to be analyzed. Each threshold mark was accurate to better than 1 db. All thresholds and amplitude measurements were made in microvolts across a 50 ohm load. The receiver response was assumed to be logarithmic between adjacent calibration marks.

Several methods were used to measure signal durations at specific thresholds. Where specular underdense signals only were measured the relative time of rise and decay at the threshold was scaled directly from the Edin chart. This information was fed into the Burroughs 220 digital

LOG AMPLITUDE

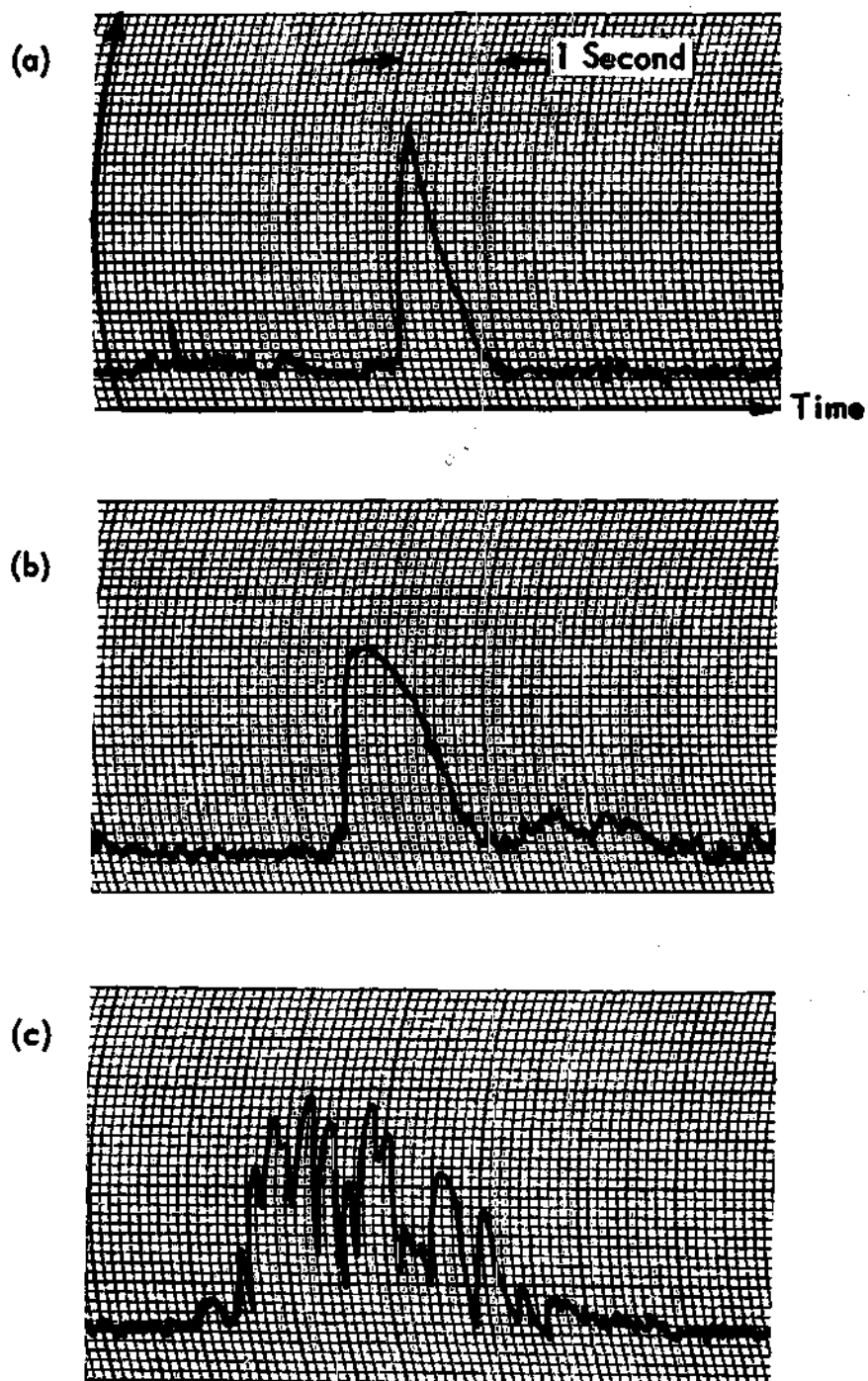


Figure 5. Examples of Three Types of Meteor Echoes:

- (a) Specular Underdense,
- (b) Specular Overdense,
- (c) Non-Specular Overdense.

computer in the form of punched cards. The computer was programmed to compute the total signal duration at each of five threshold levels. A similar method was used to find the contribution to total signal duration of the specular overdense signals. The total signal duration due to all types of signals was measured in two ways. The Edin charts were scaled manually to measure the total signal duration above each threshold. At Smyrna the UF/MSA-1 meteoric signal analyzer was used to obtain the same information automatically. This device generated constant height pulses of duration corresponding to the signal time above threshold. The pulses were integrated by a precision resistance-capacitance network. A vacuum tube voltmeter read the capacitor voltage once each hour.

The measurement of decay time constants for the specular underdense signals was a challenging problem. Since the decay is approximately exponential, a "best fit" to a true exponential of time constant τ was used. The Burroughs 220 digital computer was programmed to fit the measured signal data to an exponential by the method of least squares and then compute the time constant τ , sum of errors squared, and maximum amplitude for each set of observed data. A numerical example illustrating this computation is given in Appendix II. A set of observed values was obtained for each signal of specular underdense shape exceeding a minimum threshold at least 10 db above peak noise or background signal. Obvious distortions of the exponential decay were not entered as observed data. The computed values of τ were compared where two channels on each frequency were available. If the computed values failed to agree closely and the original signal shape revealed no obvious distortion the data were discarded. Also, the mean value of the error squared function was used as a guide to

discard poor fits to an exponential shape. It is possible that some very small time constants were omitted because of the finite system response time. In addition, some of the very large time constant signals may have been overlooked due to signal distortions and confusion with overdense signals. However, the selection procedure was deliberately planned to minimize discrimination of this sort and it is felt that the results represent a good random sample of decay time constants.

CHAPTER IV

DISCUSSION OF RESULTS

Duty cycle versus decision levels.—In Chapter II it was shown that the duty cycle dependence on receiver decision level could be expressed by

$$D_o = \frac{C_c}{kA_o^k} \quad (14)$$

The importance of the exponent k in determining the average information was given by (19) with a critical value of $k = 2$ for underdense echoes.

It is convenient to measure k using duration data by plotting D_o and A_o on log-log coordinates. If (14) is valid this plot will yield a straight line of negative slope k . The theory developed in Chapter II was based entirely on echoes from underdense trails. No attempt has been made to include the effect of overdense echoes although empirical results are presented here which include all three types of echoes.

Figures 6 through 16 show the results of measurements of duty cycle as a function of receiver decision level. The data are plotted on coordinates chosen so that a direct measurement of k can be made from the slope of a straight line. Duty cycle is expressed as a percentage of total operating time. Each figure is identified by receiver station, channel, time in 24 hour code, date, and antenna height information. Channel 49F refers to the 49.44 megacycle "fixed" antenna. The letter V is used to denote the "variable" antenna and M the "mobile" antenna. In Figures 6 through 15 the signal time was scaled from Edin data

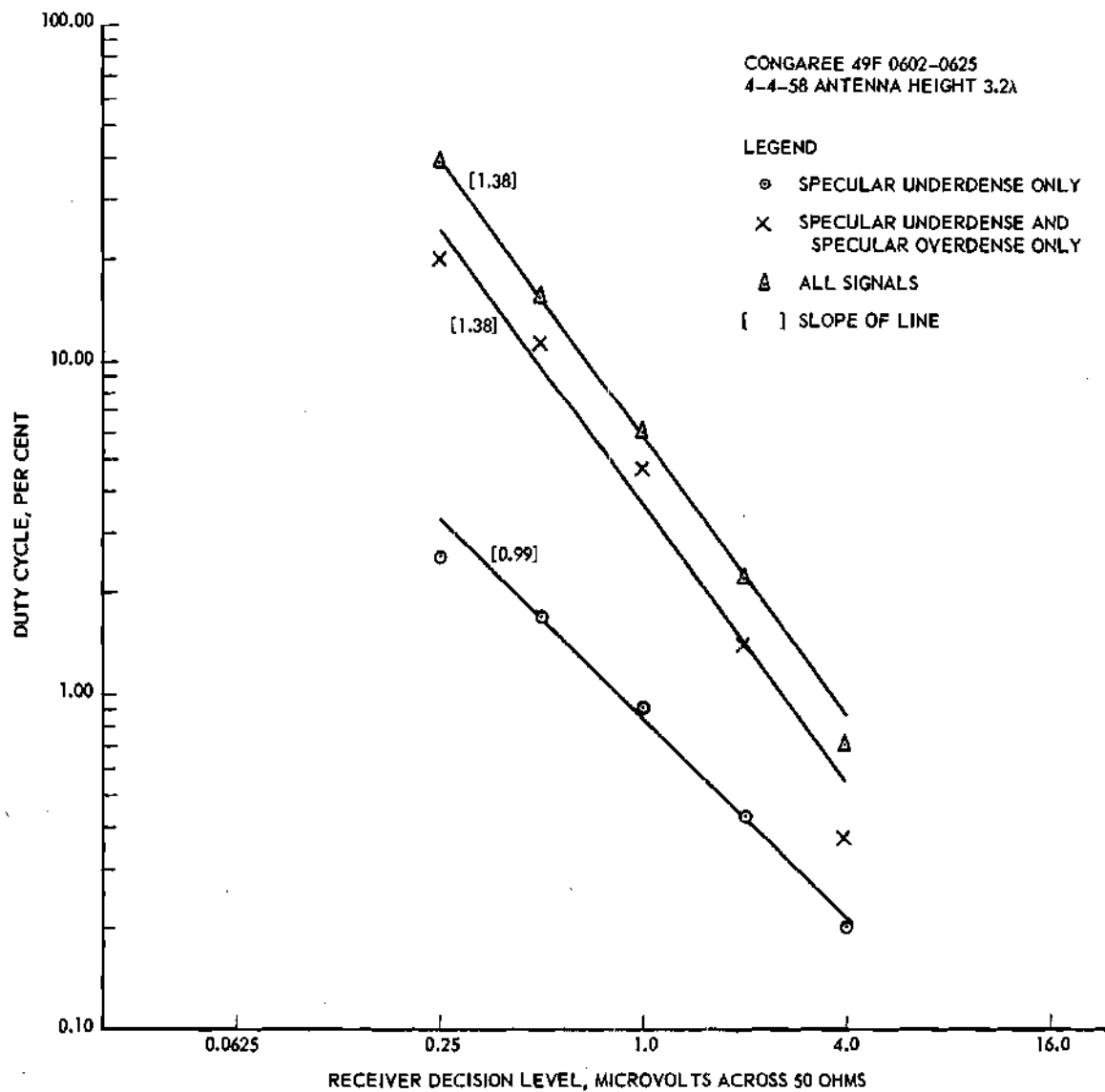


Figure 6. Duty Cycle as a Function of Receiver Decision Level as Scaled from Edin Data.

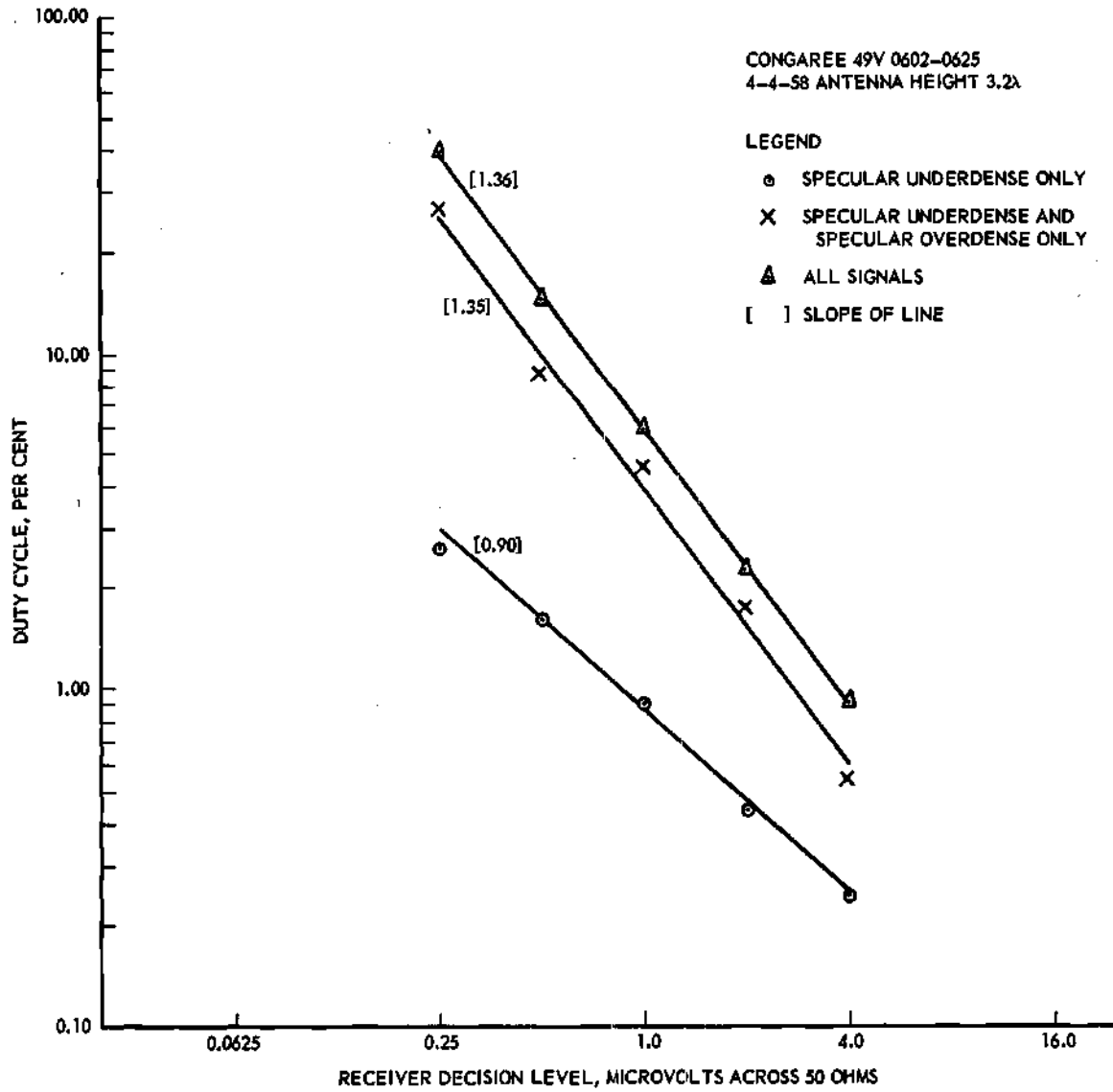


Figure 7. Duty Cycle as a Function of Receiver Decision Level as Scaled from Edin Data.

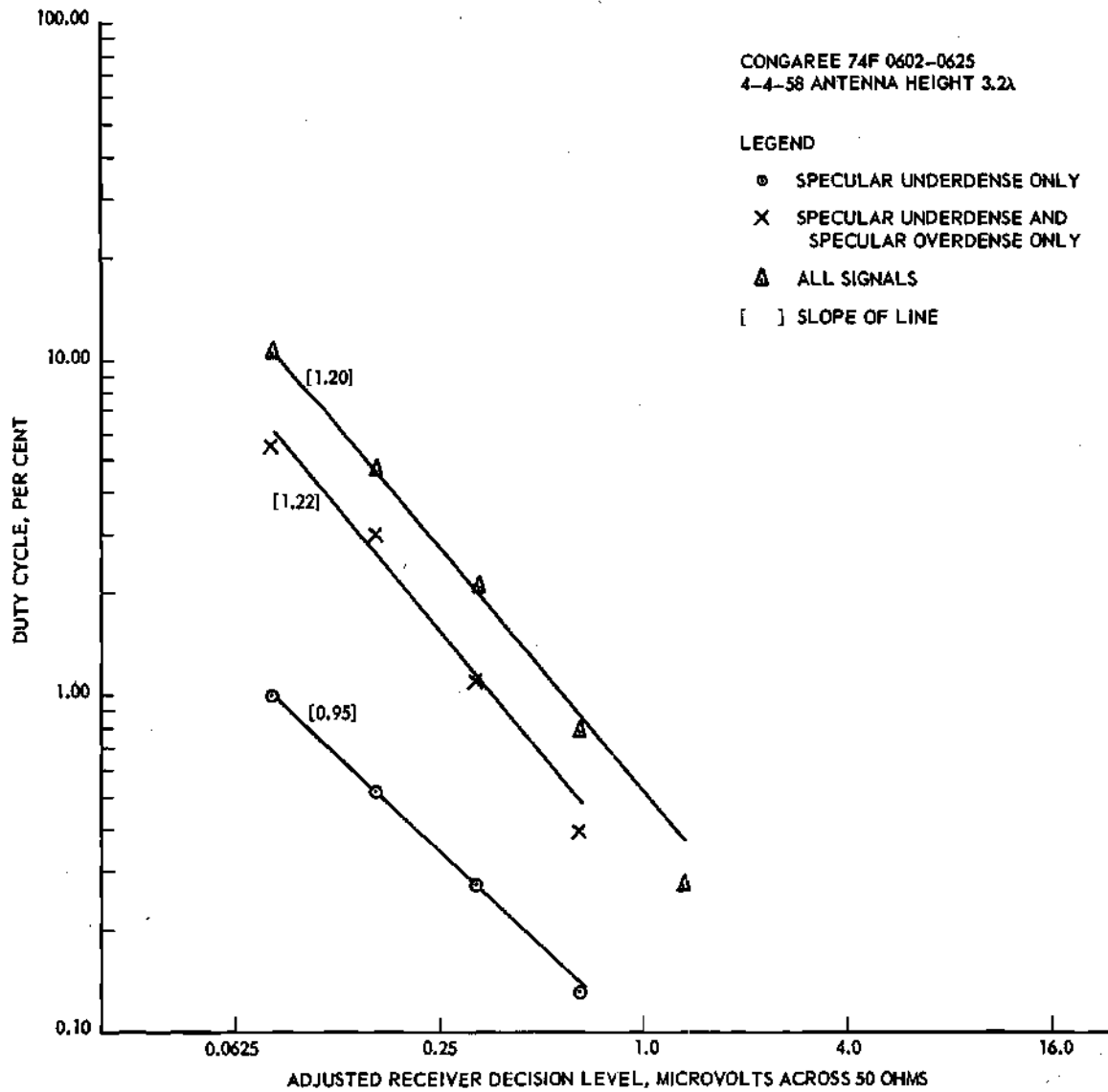


Figure 8. Duty Cycle as a Function of Receiver Decision Level as Scaled from Edin Data.

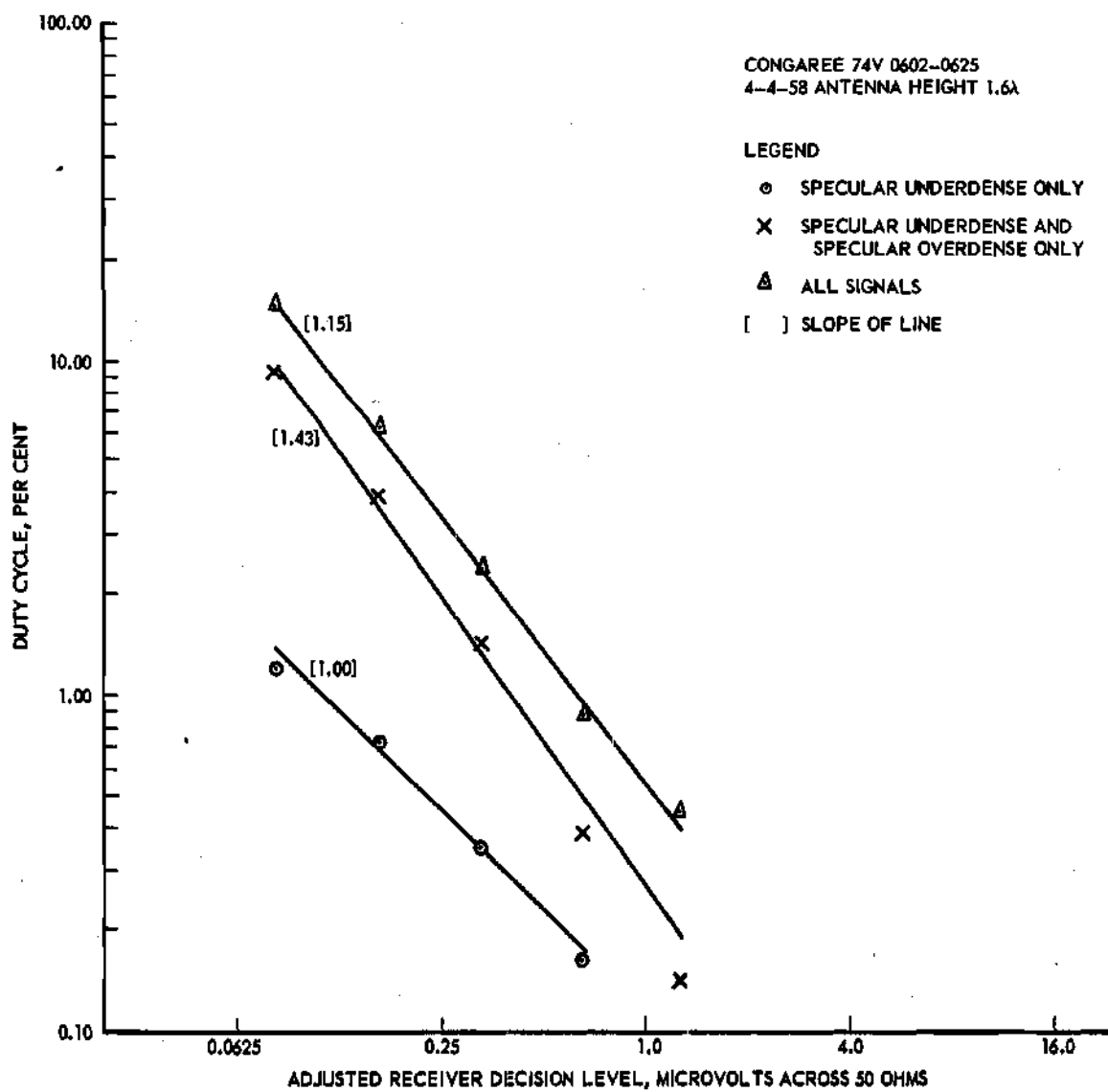


Figure 9. Duty Cycle as a Function of Receiver Decision Level as Scaled from Edin Data.

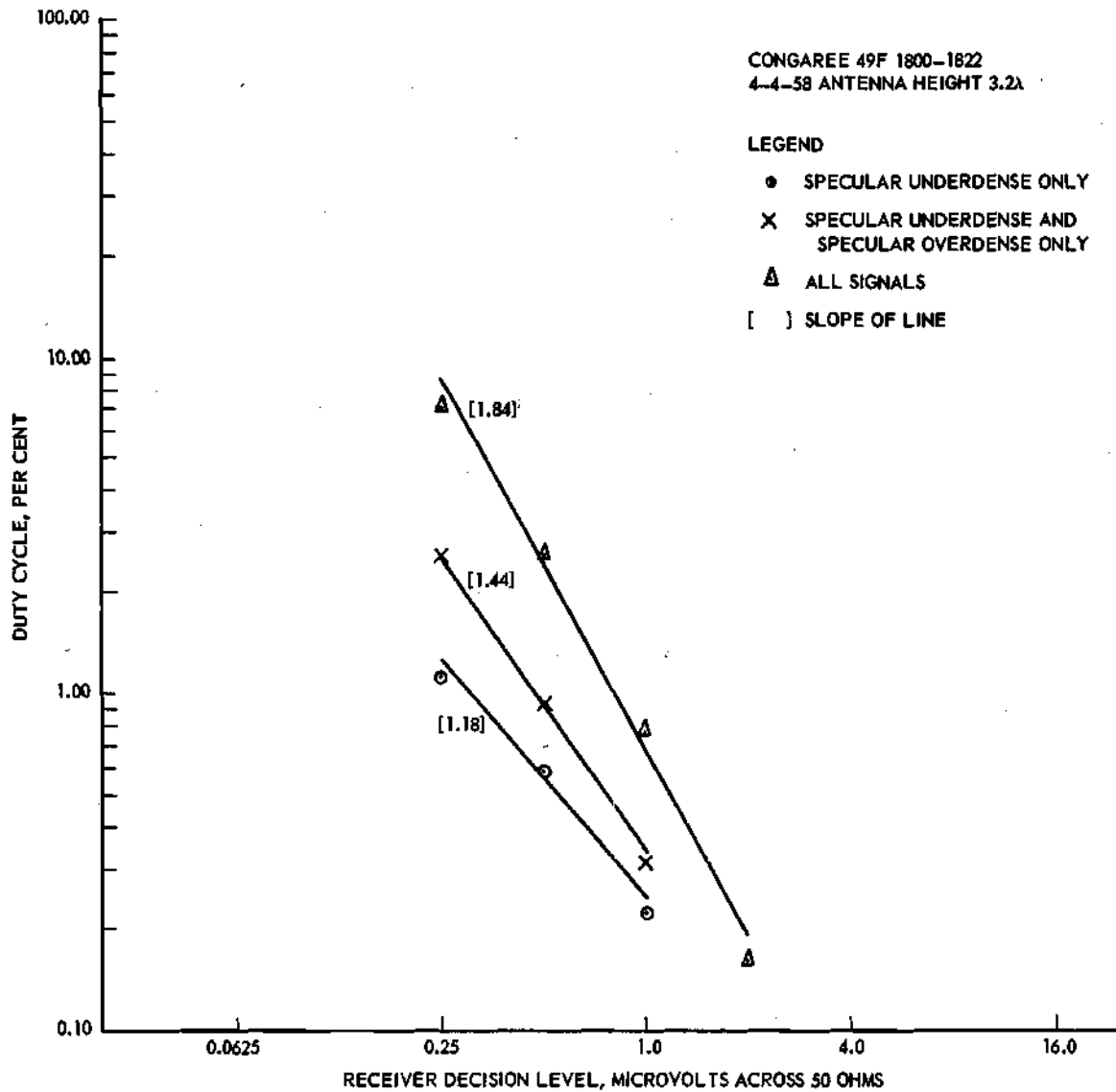


Figure 10. Duty Cycle as a Function of Receiver Decision Level as Scaled from Edin Data.

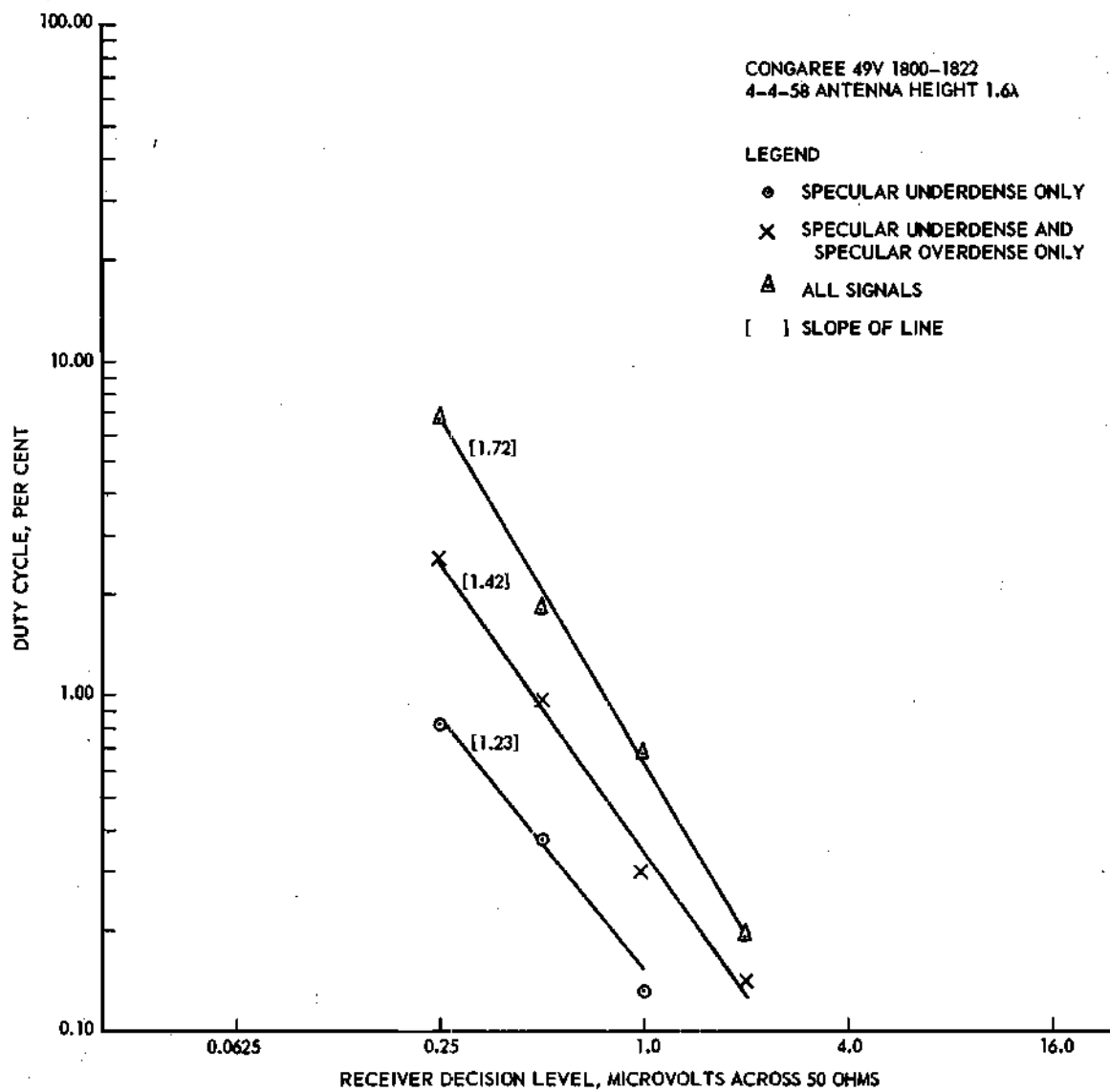


Figure 11. Duty Cycle as a Function of Receiver Decision Level as Scaled from Edin Data.

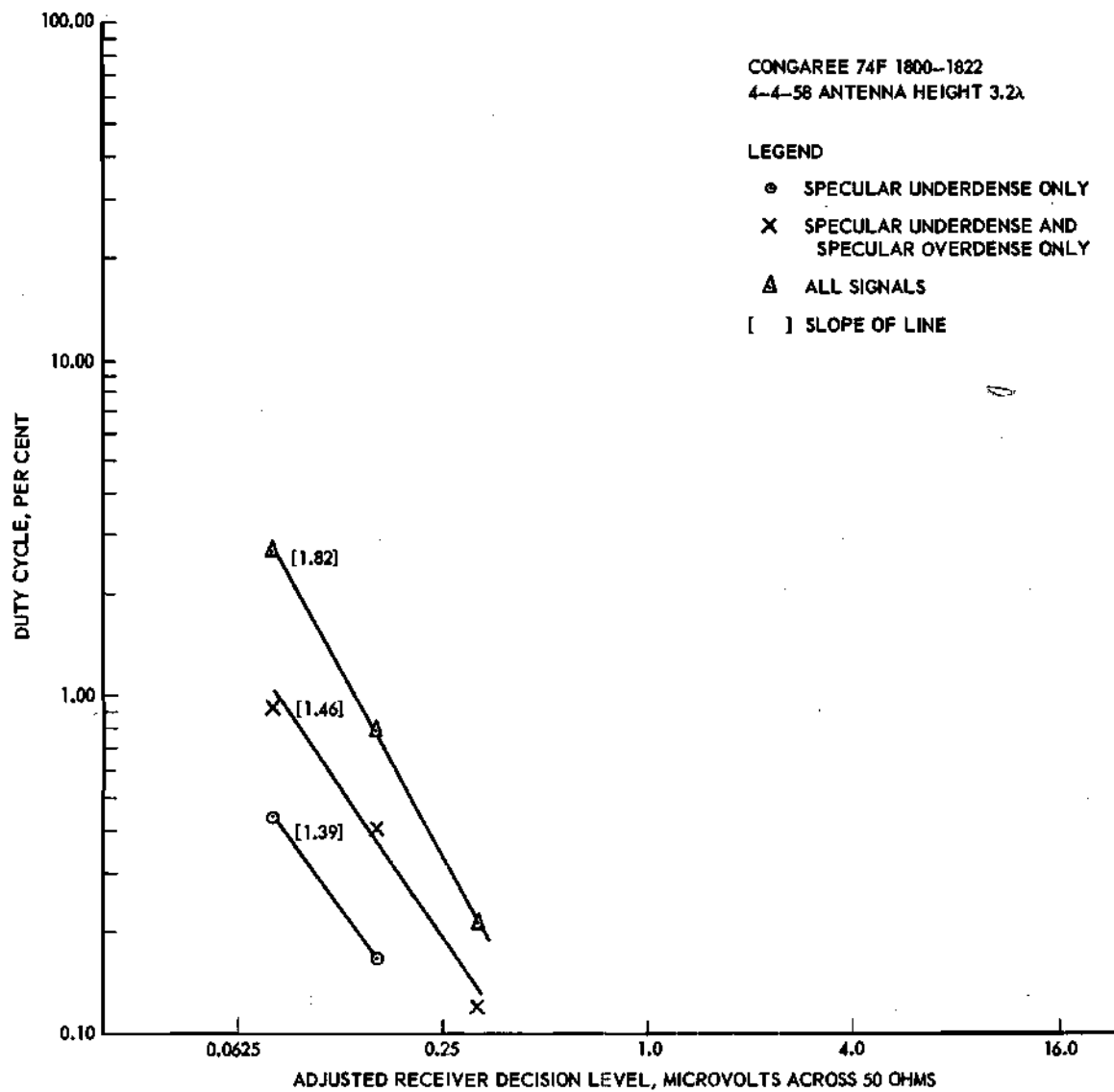


Figure 12. Duty Cycle as a Function of Receiver Decision Level as Scaled from Edin Data.

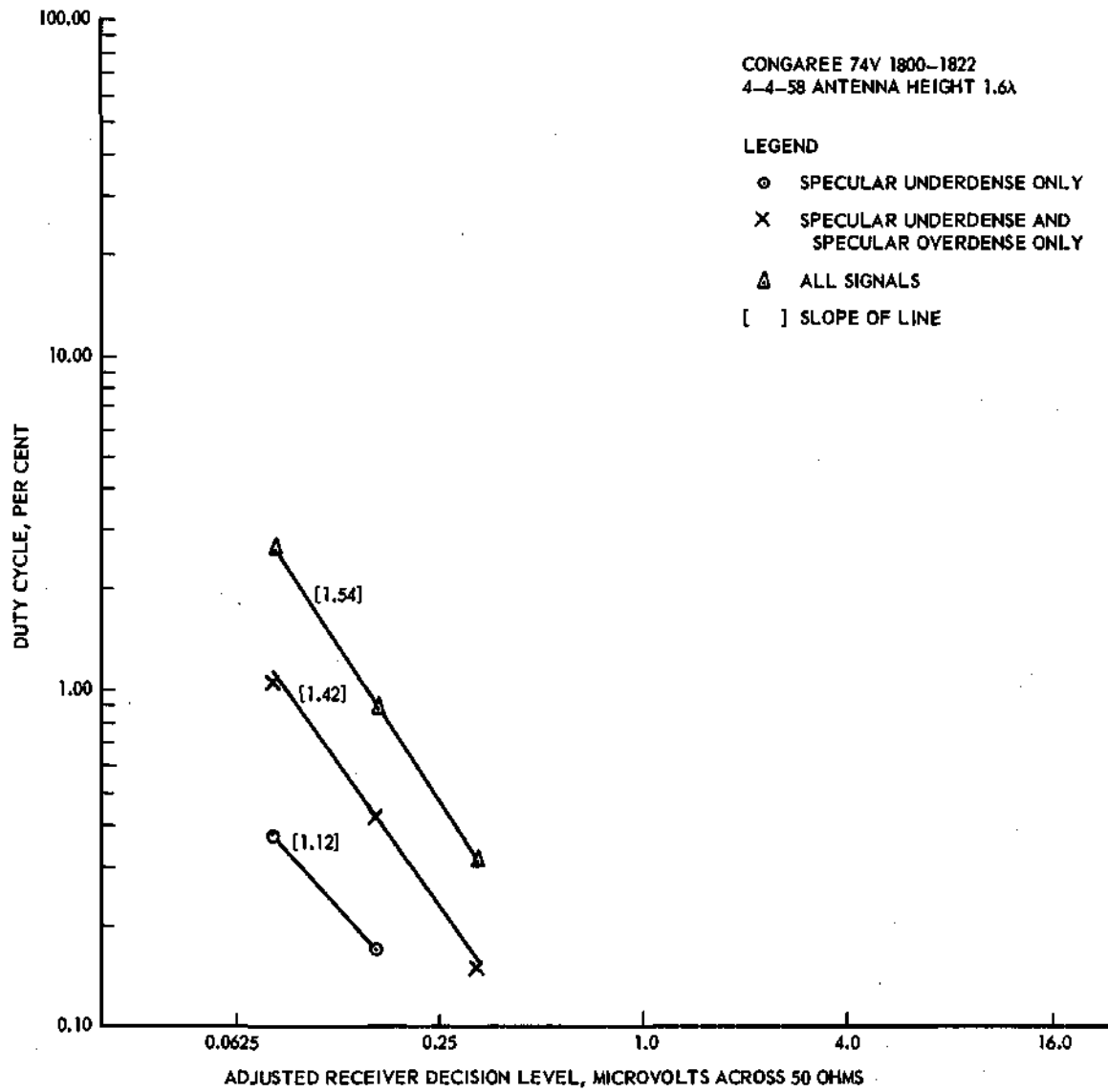


Figure 13. Duty Cycle as a Function of Receiver Decision Level as Scaled from Edin Data.

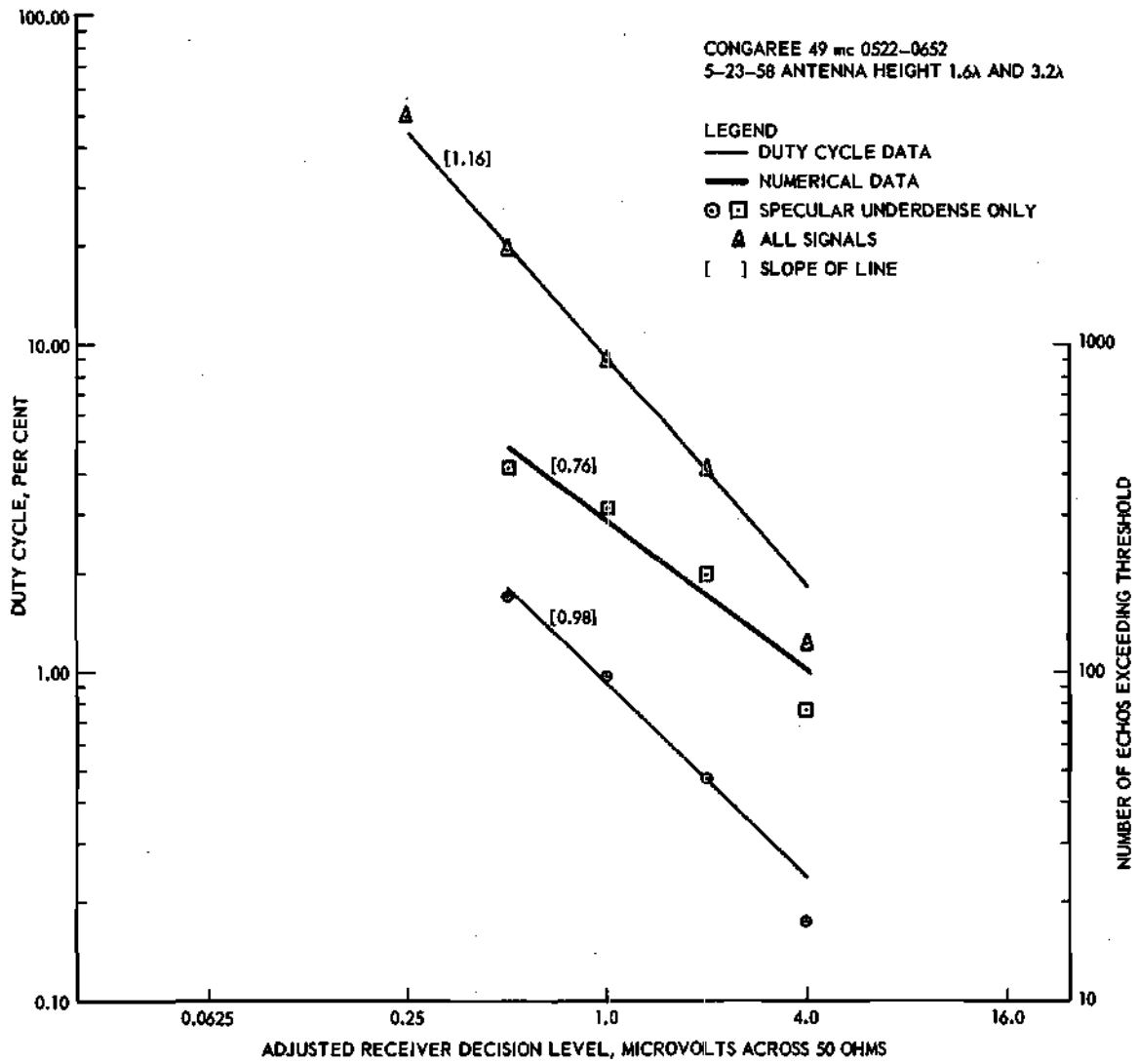


Figure 14. Comparison of Duration and Numerical Data.

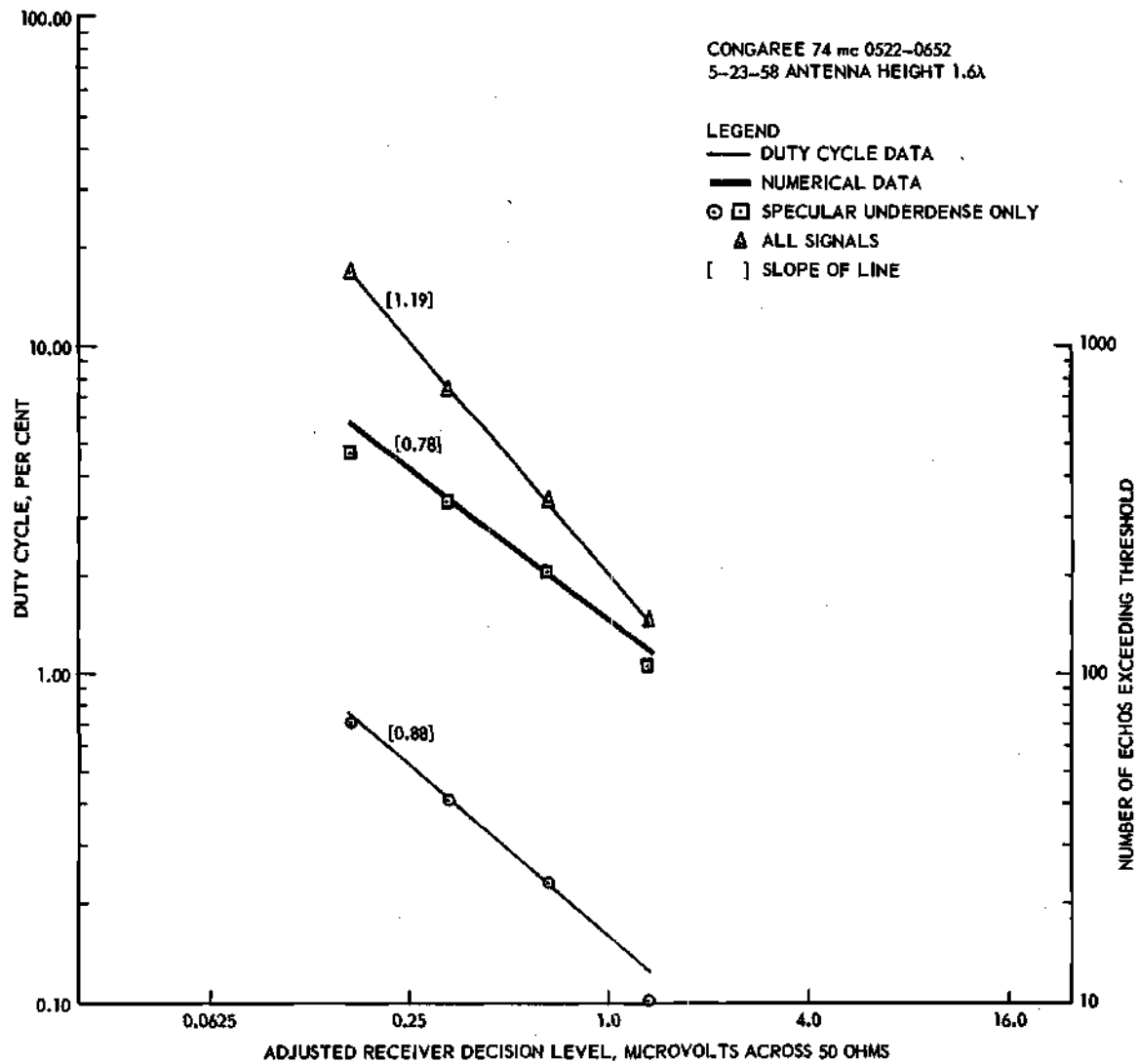


Figure 15. Comparison of Duration and Numerical Data.

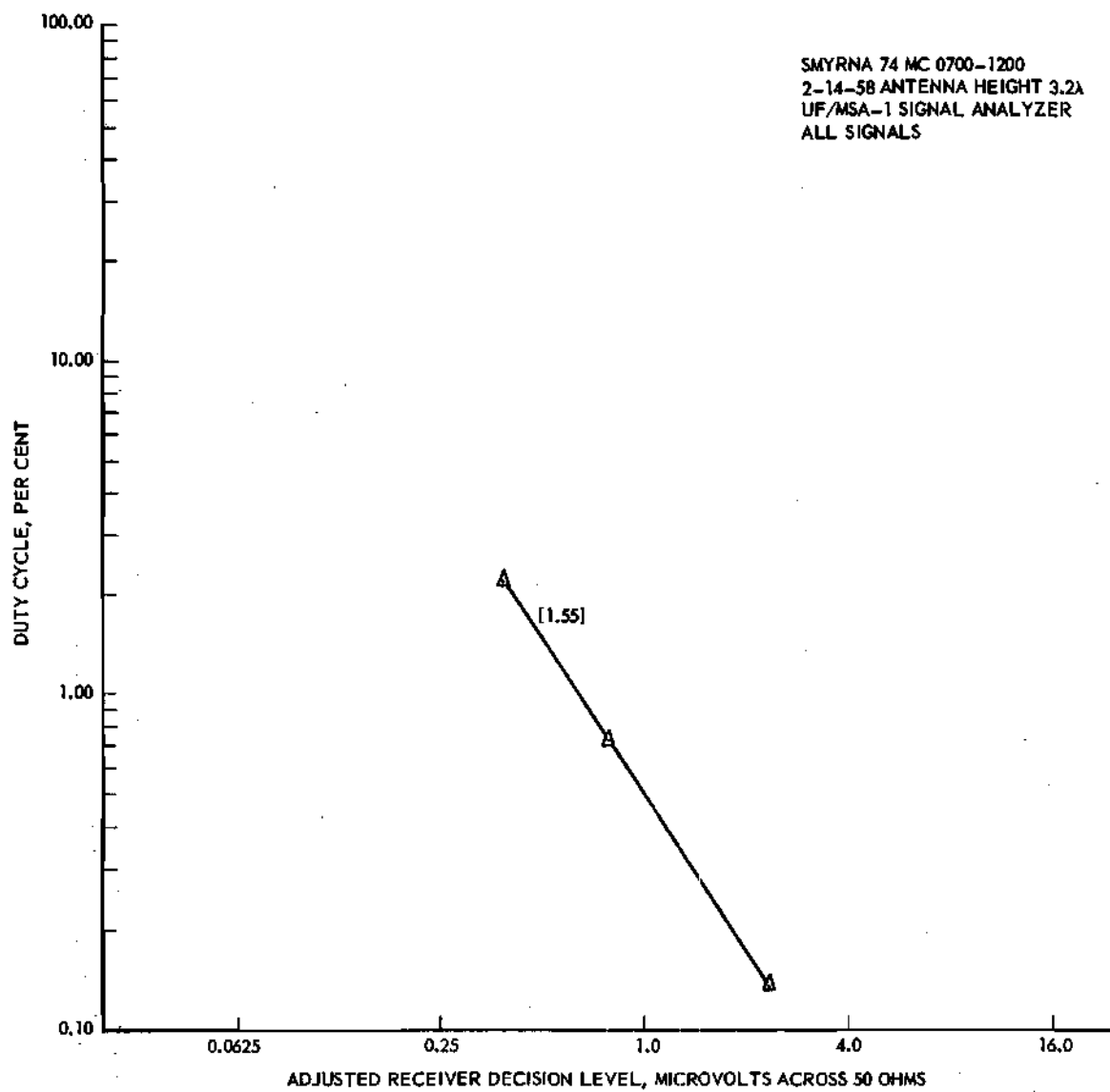


Figure 16. Duty Cycle as a Function of Receiver Decision Level as Measured by the UF/MSA-1 Meteoric Signal Analyzer.

obtained on the Walpole-Congaree radio link. All three types of signals were considered. Figure 16 was derived from operation of the UF/MSA-1 automatic signal analyzer on the Walpole-Smyrna link. This equipment did not discriminate between the three types of echoes. The receiver decision levels on 74 megacycles were adjusted to simulate a transmitted power of 5 kilowatts — the power actually used on 49 megacycles.

A straight line is fitted to each set of measurements shown although the exponential dependence has been developed for only the underdense case. It is quite possible that the inclusion of overdense signals in measurements of duty cycle should not have an exponential dependence on receiver decision level. At the signal levels used in the Walpole-Congaree and Walpole-Smyrna tests the duty cycle which considers all the signals does fit an exponential relationship very well. The straight lines as plotted cannot be extended indefinitely in either direction. At the lower thresholds the duty cycle due to meteors is limited either by receiver noise or ionospheric scatter signal. With sufficient transmitted power and low receiver noise 100% meteor-burst duty cycle can be achieved. The 100% duty cycle threshold varies with echo rate which has a strong diurnal dependence. This end of the threshold scale need not be discussed further if the exponent k has a value less than 2 since it was shown by (19) that average information rate can be maximized, in this case, by using as large a bandwidth as possible consistent with a reasonable duty cycle. The high end of the threshold cannot be extended indefinitely, either, since there must be some relatively high threshold which will, for all practical purposes, yield zero duty cycle. Also, any practicable communications system must surely

be designed about some minimum duty cycle, otherwise the problems of information storage and transmission delay become serious.

Figures 6 through 9 represent operation during a time of day of relatively high meteoric activity. Data on Figures 6 and 7 were obtained over two identical 49.44 megacycle radio systems with a common transmitting antenna and receiving antennae at the same height above a flat foreground and a lateral separation of 2.26 wavelengths. The accuracy of the duty cycle scaling technique is readily apparent from the absolute values shown on the two graphs. Figures 8 and 9 represent the 74 megacycle channels at the same time of day. In this case the antennas were at different heights above ground. Therefore, due to the difference in lobe structure, the echo correlation is poor. The duty cycle on the 1.6λ antenna (channel 74 V) is greater than the 3.2λ antenna by a factor of about 1.3. This could be caused by the fact that a height of 1.6λ gives better illumination of the meteor trail zone at the path midpoint and therefore the decay constant τ is greatest. Also, if the loci of properly oriented trails from a non-random distribution of meteors in space is considered, the illumination pattern of the 1.6λ antenna might favor a higher echo rate at this time of day. It is interesting to note that an approximate calculation based on the 1.6λ height also gives a rate factor advantage of 1.3.¹³ It would be unfair not to point out that a 2.3 db system calibration error could lead to the same result. However, as discussed in Chapter III the probable calibration error is only 1 db therefore some of the duty cycle advantage of the 1.6λ antenna height must be attributed to the more favorable antenna illumination pattern.

The specular underdense data fit the exponential law well with the exception of the measurements at the lowest threshold, which consistently gave a somewhat low duty cycle. This effect was noted on almost all of the observed data. A careful check of the Edin charts indicated that this was probably caused by multipath fading which is more prominent after an echo has persisted for some time. In some cases the observed data do not fit closely at the highest threshold. This effect is more apparent at values of duty cycle less than about 0.25%. The statistics become rather poor at this threshold with only a few very strong echoes contributing to the result.

The slopes of the lines fitted to the underdense data have a mean value of 1.06 with a probable error of 0.24. This would give a value of $k \approx 1$ for Equation (14) which is consistent with the observed mass distribution exponent of $p = 2$. The diurnal effect, if present, is very small. There is some slight increase in the slope of the lines fitted to evening data but this can neither be evaluated nor explained.

A practicable meteor-burst system will utilize echoes from overdense trails as well as underdense trails. It is possible to have the system respond only to specular echoes by taking the first derivative (with respect to time) of the echo's rise time. This is desirable to prevent activating the system on slow rise non-specular signals which have a high degree of fading and are largely uncorrelated on antennas only a few wavelengths apart. It is apparent from Figures 6 through 13 that adding specular overdense echoes to specular underdense echoes will yield a significantly higher duty cycle. The amount of increased duty cycle gained depends upon the threshold chosen because of the difference

in slopes. From Figure 6 for example at a threshold of 1.0 microvolts the specular overdense echoes will increase the duty cycle by a factor of 4.2 with a corresponding increase in average information rate. A simple threshold operated system utilizing all signals would give an additional increase by a factor of 1.7 with much greater chance for errors and a loss of privacy.

The mean value of the slopes of the specular underdense plus specular overdense lines is 1.37 with a probable error of 0.34. Again there is no apparent diurnal variation although the slopes are slightly greater in the evening. The slope of this line does not correspond to the exponent k in Equation (14) but it can be used in the bandwidth considerations implied by (19). Once again the empirical value is less than the critical value of 2 and maximum bandwidth will yield the highest average information rate.

On each of Figures 6 through 16 the duty cycle as measured from all types of signals is plotted for reference. This represents the maximum duty cycle to be obtained at any threshold. In most instances the slope of this line has the largest value of the three. The largest value measured was 1.84 (Figure 10). It appears that this line has a significant increase in slope during the early evening hours. This effect was noticed by Vincent, et al., who, however, got the opposite result.⁴ The range of values encountered during this experiment never exceeded 2. Figure 16 shows the duty cycle as measured electronically on the Walpole-Smyrna link. A median slope value of 1.55 was obtained over a prolonged run of 5 hours. It is significant that the absolute

values obtained at Smyrna agree very closely with values scaled from Edin charts taken at Congaree two months later.

Figures 14 and 15 compare the values of k as determined from both duration and rate data. The rate relationship is given in Chapter II by

$$N_o = \frac{C}{A_o k} \quad (8)$$

which when plotted on log-log coordinates will yield a straight line of negative slope k . This was done and is presented in Figures 14 and 15 for the 49 megacycle and 74 megacycle channels respectively together with simultaneous measurements of duty cycle. It appears that the value of k as determined from the numerical (rate) data is somewhat lower than that measured by the duration data. A possible explanation for this discrepancy is that the specular underdense signals were counted primarily in connection with a measurement of the distribution of decay time constants. Only clearly defined echoes were counted and this tends to discriminate against the counts at lower thresholds where multiple signals are more frequent.

A comparison of duty cycle on the two frequencies can easily be made by examination of Figures 6 through 13. If only underdense signals are considered the duty cycle will be a function of λ^5 , since

$$P_R = P_{TIR} G_T G_R \lambda^3 q^2 \text{ and } \tau = \frac{\lambda^2 \sec^2 \theta}{16 \pi^2 D} .$$

Then the average duration will

depend on $\lambda^3 \cdot \lambda^2 = \lambda^5$ when both channels detect the same echo with equal transmitted power, antenna gains, and receiver decision level. For the frequencies used here λ^5 is equal to approximately 7.6. The mean ratio scaled from data presented in Figures 6 through 13 is 9.3 which

differs from theory by a factor less than the probable calibration error in each system.

Distribution of decay constants.—Figures 17 through 20 show the distribution of meteor echo decay time constants τ for each frequency at two critical times of day. As discussed in Chapter II, the shape of this distribution is closely related to the distribution of meteor velocities. Figures 17 and 18 were obtained from morning data (0400 - 0900 EST). At this time of day the earth's heliocentric velocity vector adds to the meteor's heliocentric velocity vector to give relatively higher geocentric velocities. During the early evening the meteor trail zone is at the earth's antapex and relatively lower geocentric velocities are encountered. The evening data are presented in Figures 19 and 20 for each frequency.

The distribution of decay constants is rather broad in all cases but this was to be expected due to the great range of velocities encountered (12 to 72 kilometers per second) and due to the exponential nature of the diffusion coefficient D which varies from about 1 to over 300 meters squared per second in the meteor trail zone. As a consequence, a relatively large number of statistics are necessary to define the shape accurately. There is no apparent double peak in this curve as might have been expected from previous measurements of the velocity distribution of sporadic meteors.^{6,7} The median time constant value is indicated on each graph.

A comparison of Figure 17 with Figure 19 and Figure 18 with Figure 20 indicates a diurnal variation in both the shape and the median value. The peak tends to become broader with a shift toward longer time constants in the evening. The median shift factor is 1.47 on 49 megacycles

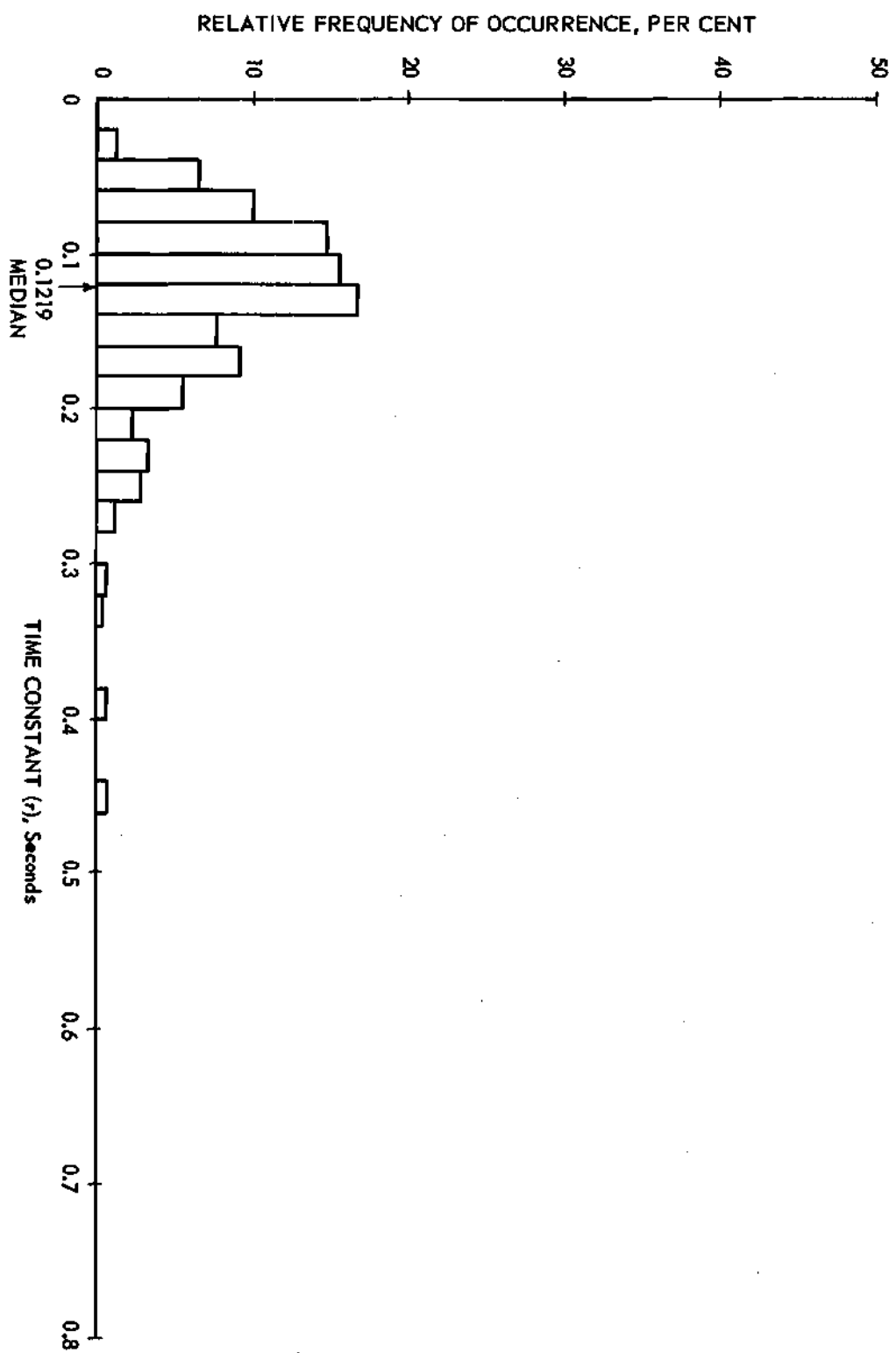


Figure 17. Distribution of Meteor Echo Decay Time Constants.
 49 mc Morning (0400 - 0900 EST), 317 Cases.

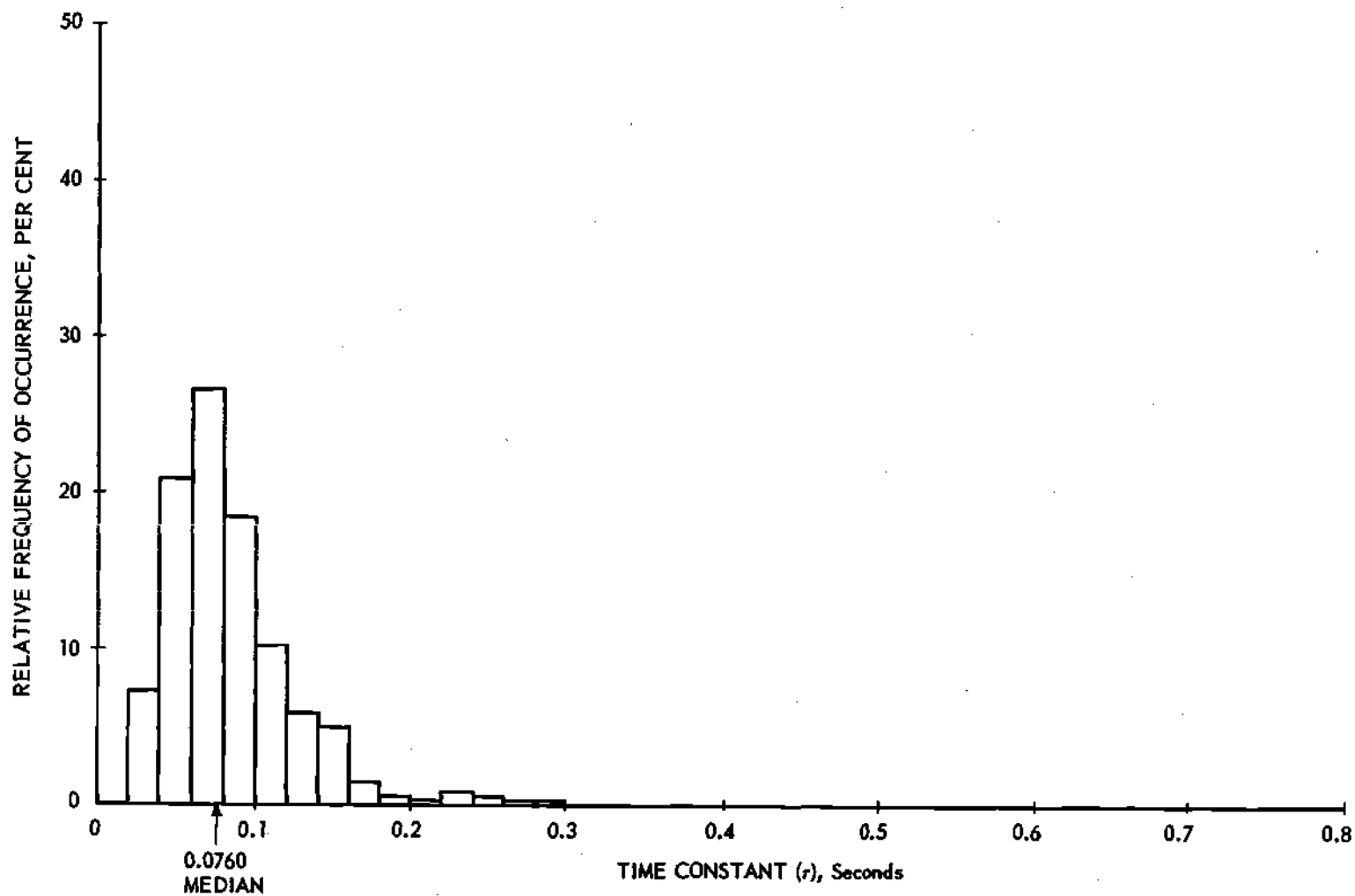


Figure 18. Distribution of Meteor Echo Decay Time Constants.
74 mc Morning (0400 - 0900 EST), 524 Cases.

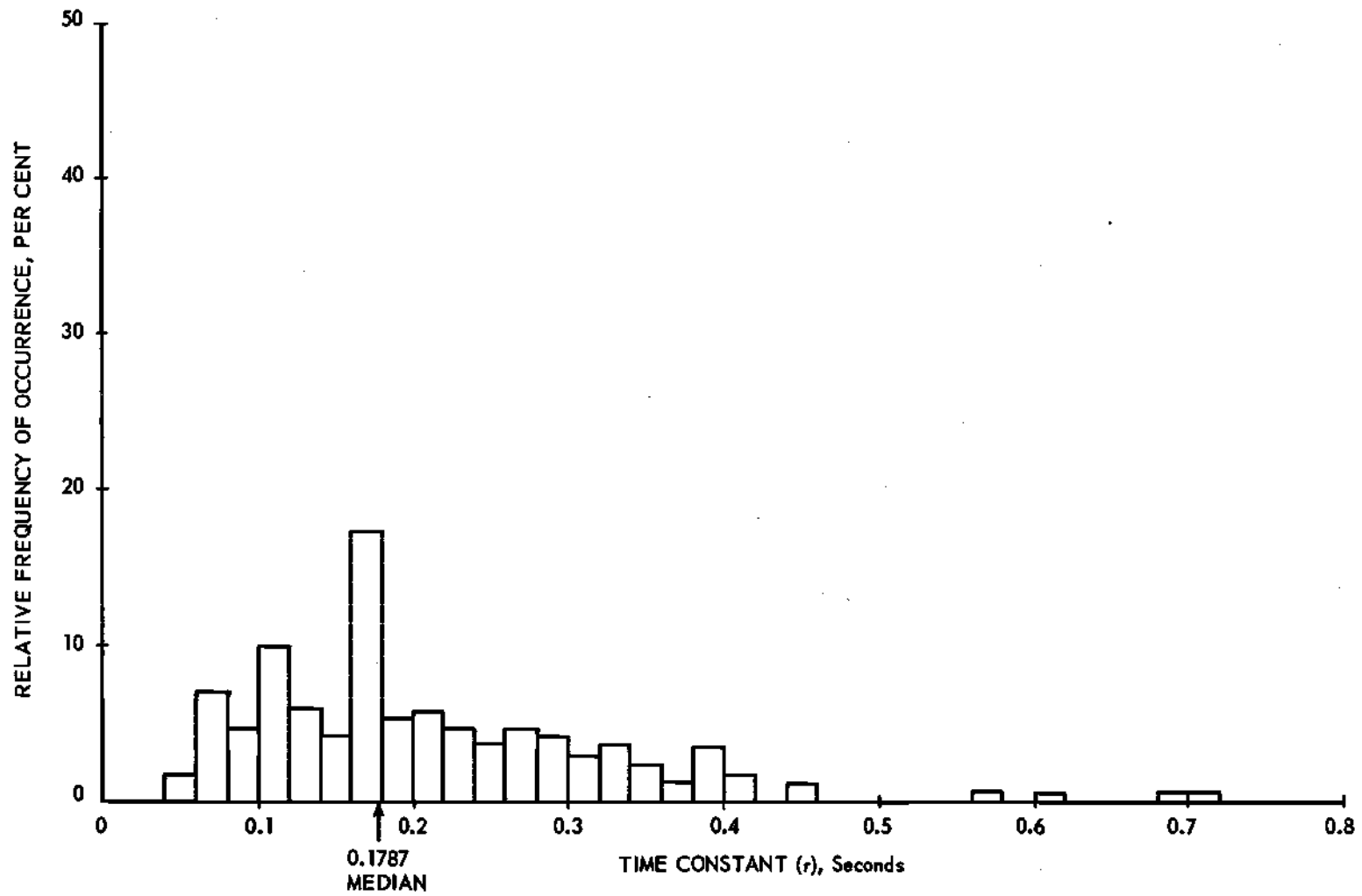


Figure 19. Distribution of Meteor Echo Decay Time Constants.
 49 mc Evening (1700 - 2000 EST), 86 Cases.

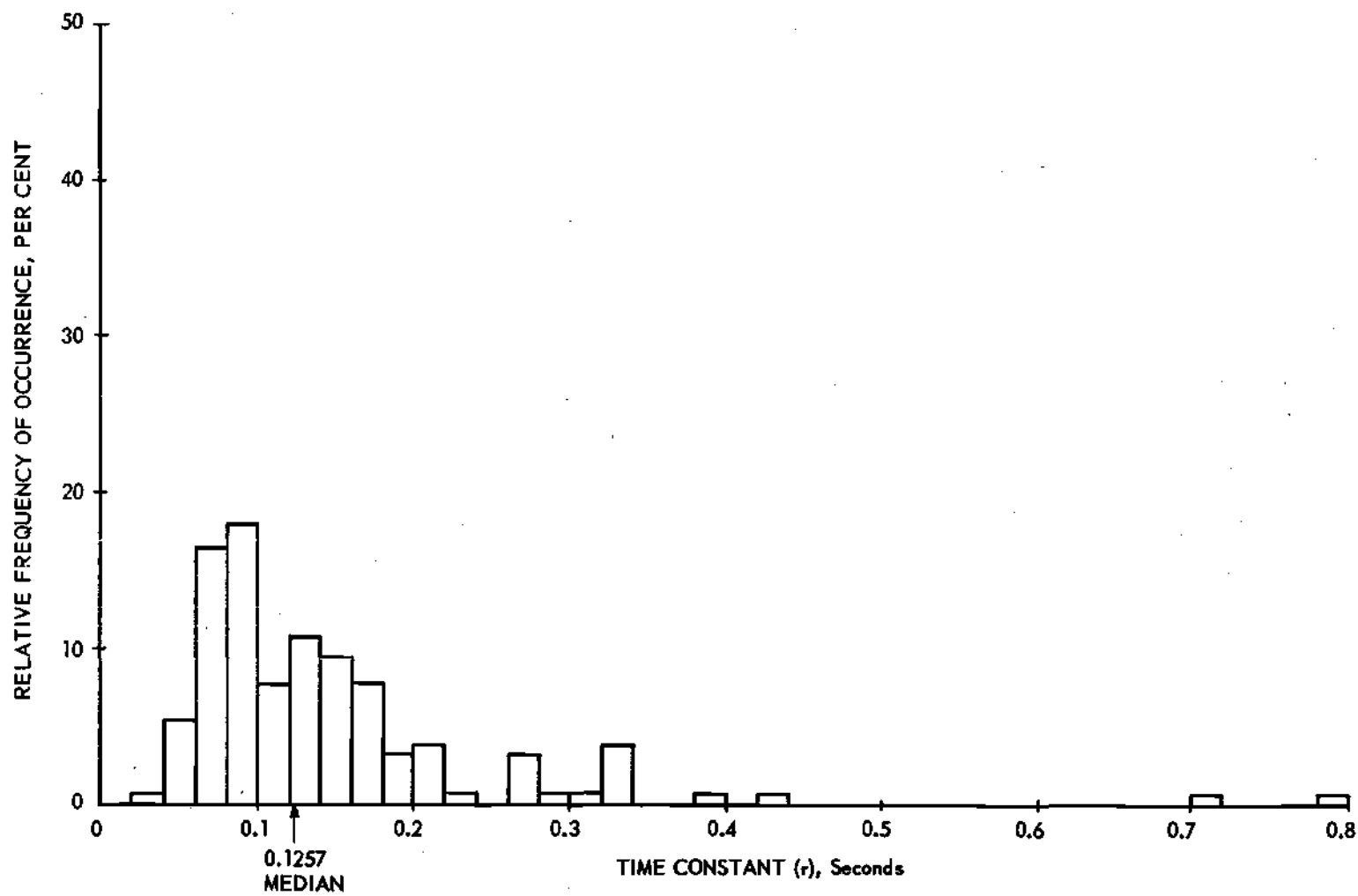


Figure 20. Distribution of Meteor Echo Decay Time Constants.
74 mc Evening (1700 - 2000 EST), 133 Cases.

and 1.65 on 74 megacycles. The statistics are much poorer in the evening due to the relatively low counting rate. This seems to contribute to the broadness of the distribution curves as can be seen by comparing Figures 19 and 20. Figure 20 with 133 cases seems to retain its overall shape better than Figure 19 which uses only 86 cases. The 74 megacycle morning data in Figure 18 shows the most consistent symmetry and represents the best statistics (524 cases).

The frequency dependence factor for τ is simply λ^2 . This has a value of 2.23 at these frequencies. Since the same echoes were used in preparing Figures 17 through 20 it would be expected that the ratio of median values could be used to confirm theory. However, the ratio as determined from the experimental median values is 1.4 for morning data and 1.6 for evening data. This cannot be judged inconsistent with theory due to the wide range of values encountered. A better test of this factor could be achieved by comparing ratios in a larger number of individual echoes. This was not within the scope of this research.

The absolute values of observed decay constants should be compared with theory and known diffusion coefficients at meteor altitudes. The time constant relationship is given by

$$\tau = \frac{\lambda^2 \sec^2 \phi}{16 \pi^2 D} \quad (22)$$

On the Walpole-Congaree link ϕ has a value of $77^\circ 42'$ for a meteor at the path midpoint at an altitude of 100 kilometers. The value of D is estimated to be 10 meters squared per second at 100 kilometers altitude. Using these values in (22) τ is computed to be 0.223 seconds on 74

megacycles and 0.334 seconds on 49 megacycles. However, the median values observed range from 0.076 to 0.126 seconds on 74 megacycles and 0.122 to 0.179 on 49 megacycles. This same discrepancy was noted by Wirth based on measurements at 43.5 megacycles.⁵ Either the majority of the radio trails occur above 100 kilometers* or some unknown effect is causing the trail to diffuse more rapidly than the published values of D would indicate.

* An altitude of 110 kilometers increases the value of D to $50 \text{ m}^2/\text{sec}$ and gives a result agreeing with these experiments.

CHAPTER V

CONCLUSIONS

The duty cycle dependence exponent k as measured on a typical meteor-burst radio link using frequencies of 49 and 74 megacycles per second has a value of approximately 1 for sporadic meteors which produce underdense trails. This value is in agreement with theory. The value of k does not appear to have a significant diurnal variation. A practicable meteor-burst system similar to the one used to gather these data and utilizing all specular meteor signals may be designed about a duty cycle dependence factor of 1.4. For a simpler system using all types of signals this factor increases to about 1.5 or more with diurnal variations. In either case the exponent does not appear to exceed a value of 2 if ionospheric scatter signals are excluded. Therefore, meteor-burst systems of this general description should be designed to utilize the maximum feasible bandwidth consistent with minimum acceptable signal-to-noise ratio and duty cycle.

The distribution of meteor echo decay time constants has been determined for a typical meteor-burst radio link. The distribution is velocity sensitive as predicted by theory. The shift in the median decay constant due to the earth's heliocentric velocity has been evaluated based on these data with a median shift factor of about 1.55 from morning to evening. The median value of the decay constant fails to agree with theory and published values of the diffusion coefficient D if the majority of trails detected by forward scatter radio occur at an altitude of 100

kilometers. The agreement becomes quite good for a median altitude of 110 kilometers or for a diffusion coefficient of 50 meters squared per second.

Figure 21 may be used to illustrate the effect of varying the frequency and bandwidth parameters on a typical meteor-burst system. Received power P_R in decibels above a one milliwatt reference level is plotted as a function of duty-cycle in per cent for each frequency. Various measured signal and noise levels are indicated by horizontal lines on the left side of the figure. These data are based on measurements and results reported herein and elsewhere.¹⁴ The values are typical for a system of good design. The 74 megacycle values of duty cycle were scaled from measured 49 megacycle data as indicated on the figure.

It has already been concluded that the maximum permissible bandwidth is desirable from an information rate standpoint. Any possible operating frequency advantage is best illustrated by a simple numerical example. Let the minimum acceptable duty cycle be 3 per cent at 0600 and the minimum acceptable signal-to-noise ratio be 10 decibels. Assume a fixed bandwidth system is to be designed for each frequency. On 49 megacycles 3 per cent duty cycle occurs at a threshold of -104 dbm. The noise plus ionospheric scatter level must not exceed -114 dbm. Since this is already the level of ionospheric scatter (PIS) at noon in the summer the receiver bandwidth can only be increased to the point where total receiver noise (N_R) just begins to affect this threshold. If ionospheric scatter signal is added in an rms manner with noise this threshold occurs about 10 db below the PIS threshold or -124 dbm. The

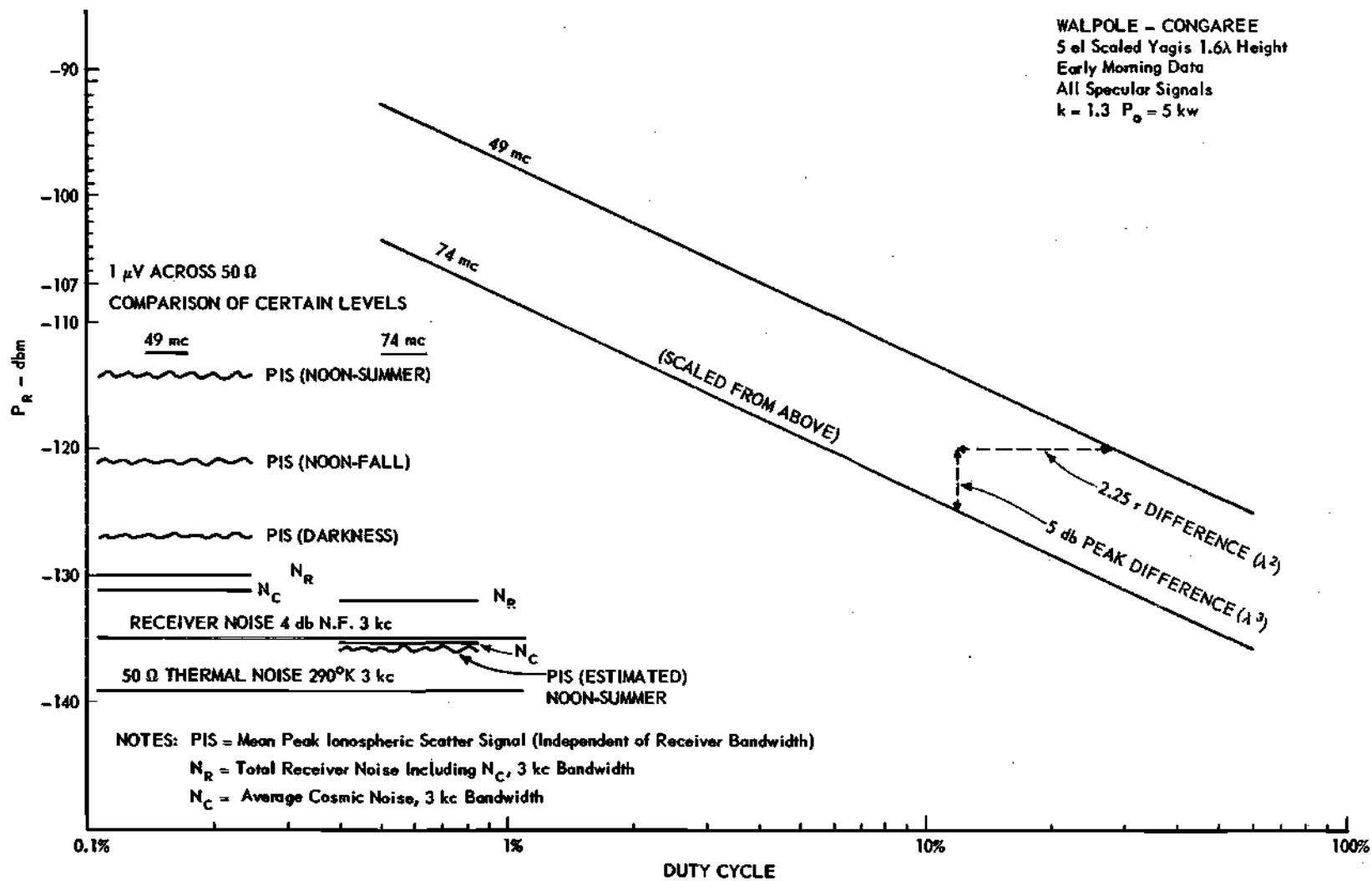


Figure 21. Bandwidth-Frequency Considerations on a Typical Meteor-Burst Radio Link.

value of N_R is -130 dbm at 3 kc bandwidth so the 49 mc bandwidth may be increased by a factor of 4 to 12 kilocycles. Similar calculations applied to the 74 mc levels also yields a bandwidth of 12 kilocycles. It may be concluded that when ionospheric scatter signal is considered as noise in a burst system the advantages of the lower frequencies in terms of stronger echoes and longer durations are sometimes lost. Of course, the dependence of ionospheric levels on solar activity has been established and can be compensated for to a large extent by varying the bandwidth to match noise and scatter signal levels.¹⁴ For example, in the case discussed above the bandwidth of the 49 megacycle system should be increased to 120 kilocycles during the darkness hours where total receiver noise is controlling. This would yield a tenfold increase in information rate over the 74 megacycle system whose bandwidth is still limited to 12 kilocycles by total receiver noise.

CHAPTER VI

RECOMMENDATIONS

The results contained in this report were determined from propagation experiments conducted over two similar radio links. The measurements were made at only two frequencies in the very-high-frequency spectrum. Data obtained over other radio links using different paths, antenna configurations, and frequencies should be analyzed to furnish information needed to extrapolate these results. A high speed digital computer program is available in universal form to determine time constants by the method of least squares. This could be used to help evaluate the distribution of echo decay constants for other propagation paths. It should be emphasized that any investigation involving the details of the echo shape requires overall system response times of the order of one-tenth of the smallest time constants of interest. The data to be analyzed must also be taken at a chart speed sufficiently high to clearly resolve the echo shape and permit accurate time measurements.

A P P E N D I X

APPENDIX I

CALCULATION OF SYSTEM RESPONSE

In Chapter III the measured response time of the overall receiving system was illustrated. It was concluded that the system response was essentially exponential over a wide range. The effect of this finite system response time on an exponentially decaying meteor signal shape is of interest. The problem is simplified by assuming the system to be an RC network with a system time constant of RC seconds. This is illustrated in Figure 22. A network of this type has an exponential transfer function.

The exponential forcing function $e(t)$ is normalized to a time constant $\tau = 1$ second. Solving for the output voltage $v_c(t)$ as a function of RC and t for $t \geq 0$ is performed by writing the circuit differential equation

$$e^{-t} = i(t)R + \frac{1}{C} \int i(t) dt \quad (23)$$

which is first solved for the transient current $i_h(t)$ in the homogeneous differential equation

$$0 = i_h(t)R + \frac{1}{C} \int i_h(t) dt . \quad (24)$$

Differentiating (24)

$$R \frac{di_h(t)}{dt} + \frac{1}{C} i_h(t) = 0 \quad (25)$$

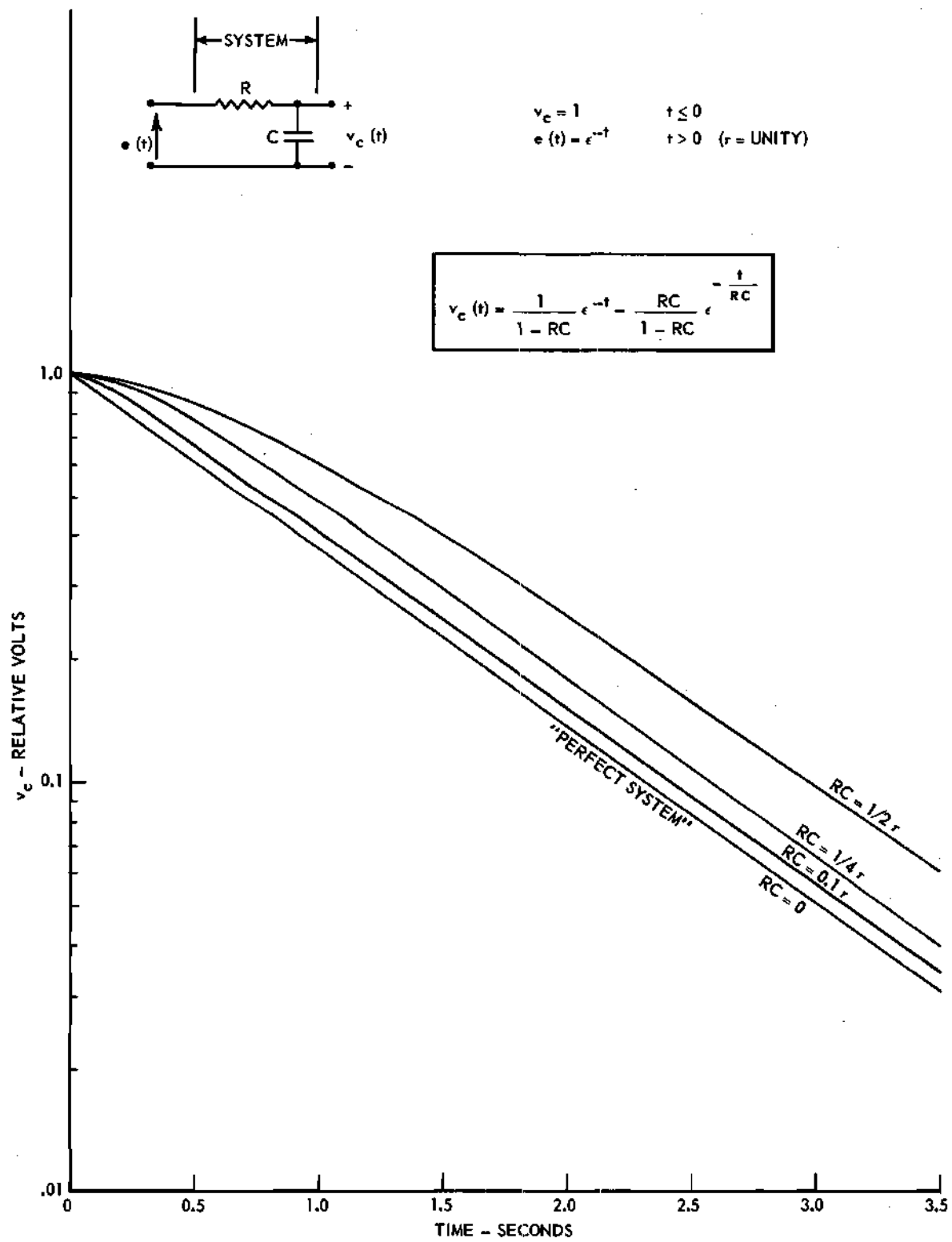


Figure 22. Theoretical Effect of Finite System Response Time on an Exponential Decay Signal.

Assume a solution of form $i_h(t) = Ae^{mt}$. Substituting in (25) and factoring

$$Ae^{mt} \left[R + \frac{1}{mc} \right] = 0 \quad (26)$$

and since $Ae^{mt} \neq 0$

$$R + \frac{1}{mc} = 0 \quad (27)$$

$$m = -\frac{1}{RC}$$

and the transient current is

$$i_h(t) = Ae^{-\frac{t}{RC}} \quad (28)$$

Solving for the steady state current $i_s(t)$

$$\varepsilon^{-t} = i_s(t)R + \frac{1}{C} \int i_s(t) dt \quad (29)$$

Assume a solution of form $i_s(t) = Be^{-t}$ which has the same frequency as the forcing function. Substituting in (29)

$$\varepsilon^{-t} = Be^{-t} R - \frac{1}{C} Be^{-t}$$

Divide by ε^{-t}

$$1 = B \left[R - \frac{1}{C} \right]$$

$$B = \frac{C}{RC - 1} \quad (30)$$

Then the steady state current becomes

$$i_s(t) = \frac{C}{RC - 1} e^{-t}. \quad (31)$$

The total current is the sum

$$i(t) = i_h(t) + i_s(t) = Ae^{-\frac{t}{RC}} + \frac{C}{RC - 1} e^{-t}, \quad (32)$$

but

$$v_c(t) = \frac{1}{C} \int i(t) dt$$

$$v_c(t) = \frac{A}{C} \int e^{-\frac{t}{RC}} + \frac{1}{1 - RC} \int e^{-t} dt \quad (33)$$

therefore

$$v_c(t) = -ARe^{-\frac{t}{RC}} + \frac{1}{1 - RC} e^{-t}. \quad (34)$$

The constant A can be found by substituting the initial condition

$$v_c(t) = 1 \text{ at } t = 0$$

or

$$1 = -AR + \frac{1}{1 - RC}, \quad t = 0. \quad (35)$$

The general solution for $v_c(t)$ is therefore

$$v_c(t) = \frac{1}{1 - RC} e^{-t} - \frac{RC}{1 - RC} e^{-\frac{t}{RC}} \quad (36)$$

This is plotted in Figure 22 for several values of RC.

APPENDIX II

SAMPLE CALCULATION BASED ON FITTING OBSERVED DATA
TO A TRUE EXPONENTIAL

It was shown in Chapter II that a specular underdense meteor echo can be approximated by the exponential

$$A = A_p e^{bt}, \quad b = -\frac{1}{\tau} \quad (37)$$

where A is the instantaneous signal amplitude, A_p is the peak amplitude, τ is the time required for the echo to decay to A_p/e , and t is the time measured from the time of A_p .

Observed echo shapes depart from the true exponential for a number of reasons. Primarily these are trail distortions, observational limitations, and system response limitations. The accuracy of an approximation to the true shape is limited by the number of observed points to be fitted. The method of least squares is the accepted method of curve fitting. The numerical example which follows is based on an actual set of observed data and serves to illustrate the procedure used to approximate an assumed true exponential.

The observed data are as follows

<u>time t_i, seconds</u>	<u>relative echo amplitude, A_i</u>
0	28
0.08	16
0.26	8
0.41	4

The four equations to be satisfied as nearly as possible are

$$28 = A_p e^{0 b} \quad (38)$$

$$16 = A_p e^{0.08 b} \quad (39)$$

$$8 = A_p e^{0.26 b} \quad (40)$$

$$4 = A_p e^{0.41 b} \quad (41)$$

As a first approximation equations (38) and (39) are satisfied exactly for

$$A_{p_0} = 28$$

and

$$b_0 = 7.$$

These values force the true exponential to pass through the two uppermost points.

A set of equations which is linear in the correction factors $(A_p - A_{p_0})$ and $(b - b_0)$ may be obtained by expanding each of Equations (38) through (41) in a generalized Taylor's series about the point A_{p_0} and b_0 and neglecting the values of $(A_p - A_{p_0})^2$ and $(b - b_0)^2$ and higher order terms that result. This is quite reasonable since if A_{p_0} and b_0 are reasonable approximations to A_p and b in the true exponential the higher order terms will be small compared to $(A_p - A_{p_0})$ and $(b - b_0)$. The general formula that results is

$$f_i = A_p e^{bt_i} - A_i = A_{p_0} e^{b_0 t_i} + \frac{\partial [A_p e^{bt_i} - A_i]}{\partial A_p} \bigg|_{A_{p_0}, b_0} (A_p - A_{p_0})$$

$$+ \frac{\partial [A_p e^{bt_i} - A_i]}{\partial b} \bigg|_{A_{p_0}, b_0} (b - b_0) = 0 \quad (42)$$

where f_i is one of the group of equations of condition with observed values A_i and t_i .

Applying formula (42) to each of the set of 4 observed points results in the following approximate equations of condition

$$f_1 = (A_p - 28) = 0 \quad (43)$$

$$f_2 = 0.571 (A_p - 28) + 1.280(b + 7) = 0 \quad (44)$$

$$f_3 = 3.460 = 0.162(A_p - 28) + 1.180(b + 7) = 0 \quad (45)$$

$$f_4 = 2.415 = 0.057(A - 28) + 0.650(b + 7) = 0 \quad (46)$$

Letting

$$u = A_p - 28$$

and

$$v = b + 7$$

Equations (43) through (46) may be written

$$1.00 u = 0 \quad (47)$$

$$0.571 u + 1.280 v = 0 \quad (48)$$

$$0.162 u + 1.180 v = 3.461 \quad (49)$$

$$0.057 u + 0.650 v = 2.415 \quad (50)$$

The most plausible values of u and v for these four equations are found by forming two "normal" equations

$$1.354 u + 0.958 v = 0.698 \quad (51)$$

$$0.958 u + 3.450 v = 5.650 \quad (52)$$

Solving (51) and (52) simultaneously

$$u = -0.790$$

$$v = 1.865$$

Thus the original estimate of A_p and b may be revised to

$$A_p' = 27.21$$

$$b' = -5.135$$

$$\tau' = 0.195 \text{ seconds.}$$

This process was readily adapted to iterative procedures as programmed on a high speed digital computer. The final values as obtained on the Burroughs 220 computer were

$$A_p = 24.155950$$

$$b = 4.6324171$$

$$\tau = 0.21587002$$

sum of errors squared = 3.3580312.

BIBLIOGRAPHY

1. Forsyth, P. A., Vogan, E. L., Hansen, D. R. and Hines, C. O., "The Principles of JANET -- A Meteor Burst Communication System." Proceedings of the Institute of Radio Engineers, Vol. 45, December, 1957; pp 1642 - 1657.
2. Vincent, W. R., Wolfram, R. T., Sifford, B. M., Jaye, W. E., and Peterson, A. M., "A Meteor-Burst System for Extended Range VHF Communication," Proceedings of the Institute of Radio Engineers, Vol. 45, December, 1957; pp 1693 - 1700.
3. Bliss, W. H., Wagner, R. J., Jr., and Wickizer, G. S., "Experimental Facsimile Communication Utilizing Intermittent Meteor Ionization," Proceedings of the Institute of Radio Engineers, Vol. 45, December, 1957; pp 1734 - 1735.
4. Vincent, W. R., Wolfram, R. T., Sifford, B. M., Jaye, W. E., and Peterson, A. M., "Analysis of Oblique Path-Meteor Propagation Data from the Communication Viewpoint," Proceedings of the Institute of Radio Engineers, Vol. 45, December, 1957; pp 1701 - 1707.
5. Wirth, W. J., Preliminary Observations of Forward Scattering of Electromagnetic Wave by Meteor Trails, U. S. Navy Electronics Laboratory, San Diego, California, Research Report 690, May 9, 1956.
6. Watson, F. G., Between the Planets, Revised Edition, Harvard University Press, 1956.
7. Lovell, A. C. B., Meteor Astronomy, Oxford University Press, London, 1954.
8. Whipple, Fred L., Hawkins, Gerald S., "Meteors," Handbuch Der Physik, Vol. 52, Springer-Verlag, Berlin · Gottingen · Heidelberg, 1959; pp 519 - 564.
9. Herlofson, N., "The Theory of Meteor Ionization," The Physical Society Reports on Progress in Physics, Vol. 11, 1948; p 444.
10. Eshleman, V. R., and Manning, L. A., "Radio Communication by Scattering from Meteoric Ionization," Proceedings of the Institute of Radio Engineers, Vol. 42, March, 1954; pp 530 - 536.
11. Campbell, L. L., and Hines, C. O., "Bandwidth Considerations in a JANET System," Proceedings of the Institute of Radio Engineers, Vol. 45, December, 1957; pp 1658 - 1660.

12. Loewenthal, Morton, On Meteor Echoes from Underdense Trails at Very High Frequencies, Massachusetts Institute of Technology, Lincoln Laboratory, Lexington, Massachusetts, Group 33, under Air Force Contract Number AF 19(122)-458, Technical Report No. 132, December 13, 1956.
13. Meeks, M. L., James, J. C., Berry, J. B., Jr., and Taylor, John, Studies of Meteor-Burst Propagation at 49 and 74 Megacycles, Georgia Institute of Technology, Atlanta, Georgia, Engineering Experiment Station, under Air Force Cambridge Research Center Contract Number AF 19(604)-1593, Final Report, June, 1958.
14. Berry, J. B., Jr., Monitoring and Recording of Electromagnetic Wave Transmissions, Georgia Institute of Technology, Atlanta, Georgia, Engineering Experiment Station, under Air Force Cambridge Research Center Contract Number AF 19(604)-1593, Technical Report No. 1, December, 1957.